

“Relativistic Nuclear Physics and Quantum Chromodynamics”

XXII International Baldin Seminar on High Energy Physics Problems

15th - 20th September 2014

JINR - Dubna (RUSSIA)



The PANDA Project @ FAIR

Marco Maggiora on behalf of the PANDA Collaboration

Department of Physics and INFN – Turin, Italy

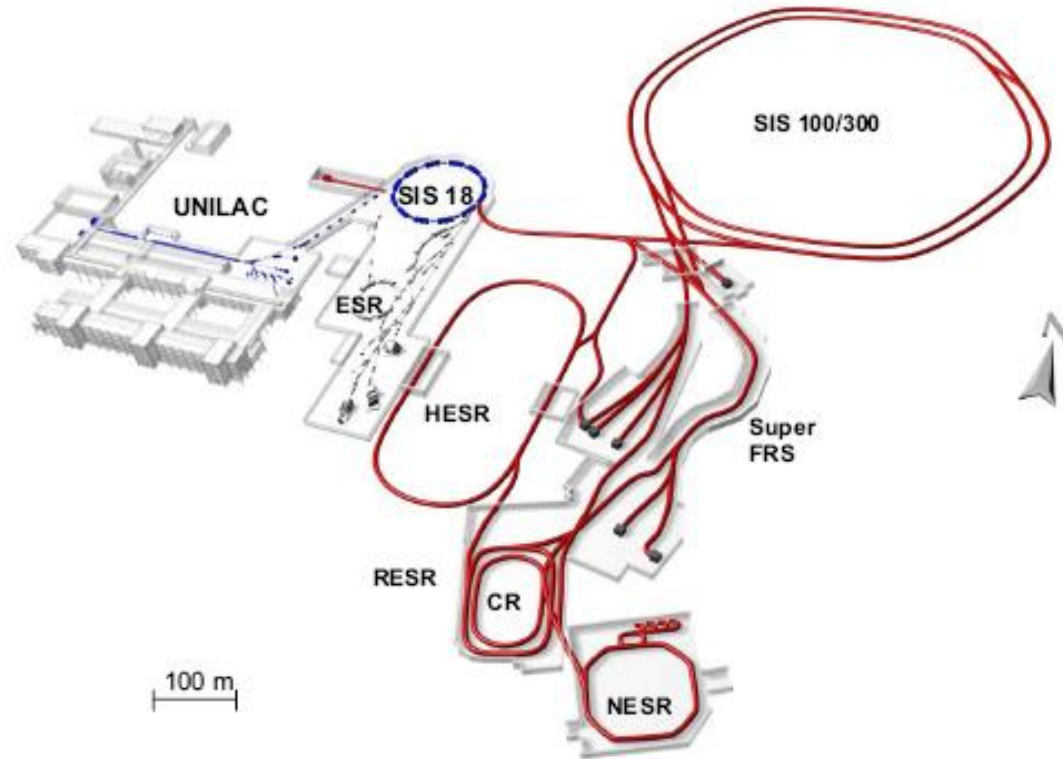




The future FAIR facility



Facility for Antiproton and Ion Research



Key Technical Features

- Cooled beams
- Rapidly cycling superconducting magnets

Primary Beams

- $10^{12}/\text{s}$; 1.5 GeV/u; $^{238}\text{U}^{28+}$
- Factor 100-1000 present in intensity
- $2(4)\times 10^{13}/\text{s}$ 30 GeV protons
- $10^{10}/\text{s}$ $^{238}\text{U}^{73+}$ up to 25 (- 35) GeV/u

Secondary Beams

- Broad range of radioactive beams up to 1.5 - 2 GeV/u; up to factor 10 000 in intensity over present
- Antiprotons 3 (0) - 30 GeV

Storage and Cooler Rings

- Radioactive beams
- e – A collider
- 10^{11} stored and cooled 0.8 - 14.5 GeV antiprotons



HESR - High Energy Storage Ring



- Production rate $2 \times 10^7/\text{sec}$

- $P_{\text{beam}} = 1 - 15 \text{ GeV}/c$

- $N_{\text{stored}} = 5 \times 10^{10} \bar{p}$

- Internal Target

High resolution mode

- $\delta p/p \sim 10^{-5}$ (electron cooling)

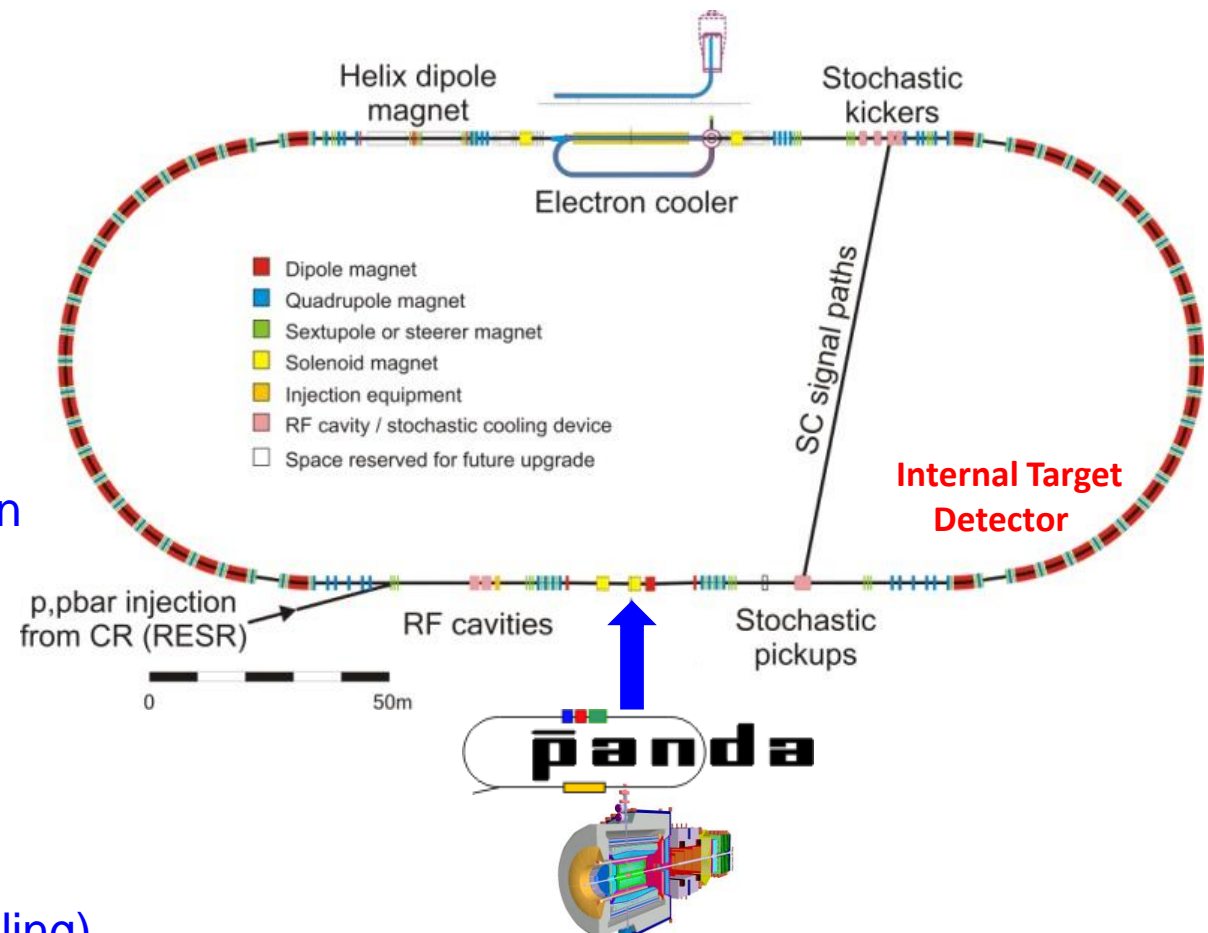
- Lumin. = $10^{31} \text{ cm}^{-2} \text{ s}^{-1}$

High luminosity mode

- Lumin. = $2 \times 10^{32} \text{ cm}^{-2} \text{ s}^{-1}$

- $\delta p/p \sim 10^{-4}$ (stochastic cooling)

$2.3 \leq \sqrt{s} \leq 5.5 \text{ GeV}$



At present 520 physicists from 67 institutions in 17 countries



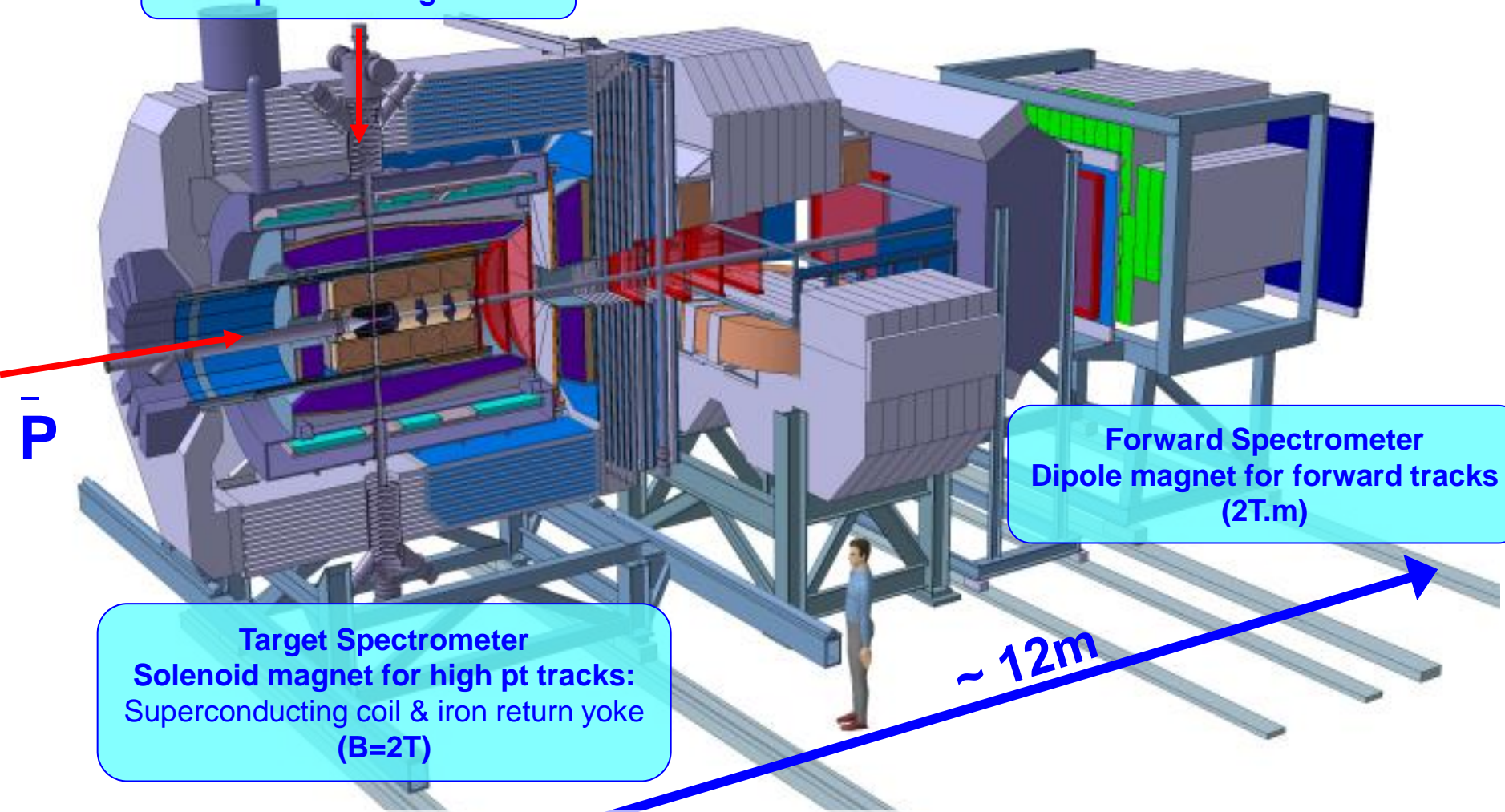
AMU Aligarh, Basel, Beijing, BITS Pillani, Bochum, IIT Bombay, Bonn, Brescia, IFIN Bucharest, IIT Chicago, AGH-UST Cracow, JGU Cracow, IFJ PAN Cracow, Cracow UT, Edinburgh, Erlangen, Ferrara, Frankfurt, Gauhati, Genova, Giessen, Glasgow, GSI, FZ Jülich, JINR Dubna, Katowice, KVI Groningen, Lanzhou, Legnaro, LNF, Lund, Mainz, Minsk, ITEP Moscow, MPEI Moscow, TU München, Münster, BARC Mumbai, Northwestern, BINP Novosibirsk, IPN Orsay, Pavia, IHEP Protvino, PNPI St.Petersburg, South Gujarat University, SVNIT Surat, Sadar Patel University, KTH Stockholm, Stockholm, FH Südwestfalen, Suranaree University of Technology, Sydney, Dep. A. Avogadro Torino, Dep. Fis. Sperimentale Torino, Torino Politecnico, Trieste, TSL Uppsala, Tübingen, Uppsala, Valencia, NCBJ Warsaw, TU Warsaw, AAS Wien



PANDA spectrometer



$\bar{p}p$: Pellet or Cluster target
 $\bar{p}A$: wire target



Physics Performance Report for PANDA arXiv:0903.3905 [hep-ex]

PANDA Magnet TDR http://www-panda.gsi.de/archive/public/P_magn_TDR.pdf

15-20 Sep 2014

ISHEPP2014



Target system

- Requirements

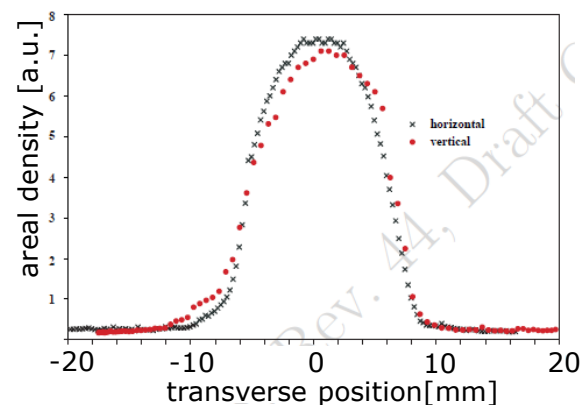
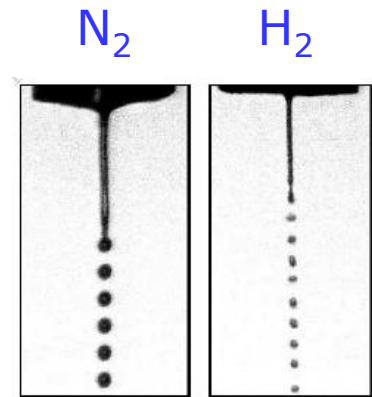
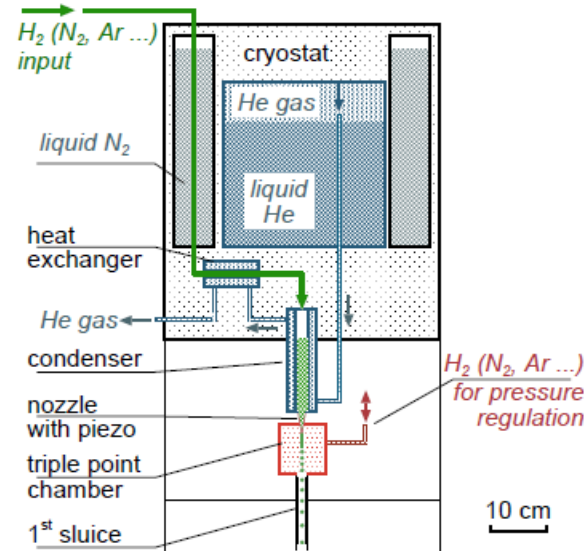
- Proton Target
- $5 \times 10^{15} \text{ cm}^{-2}$ for maximum luminosity

- Pellet Target

- Frozen droplets $\varnothing 20\mu\text{m}$
- also possible: $\text{D}_2, \text{N}_2, \text{Ne}, \dots$
- Status: $\rho \sim 5 \times 10^{15}$

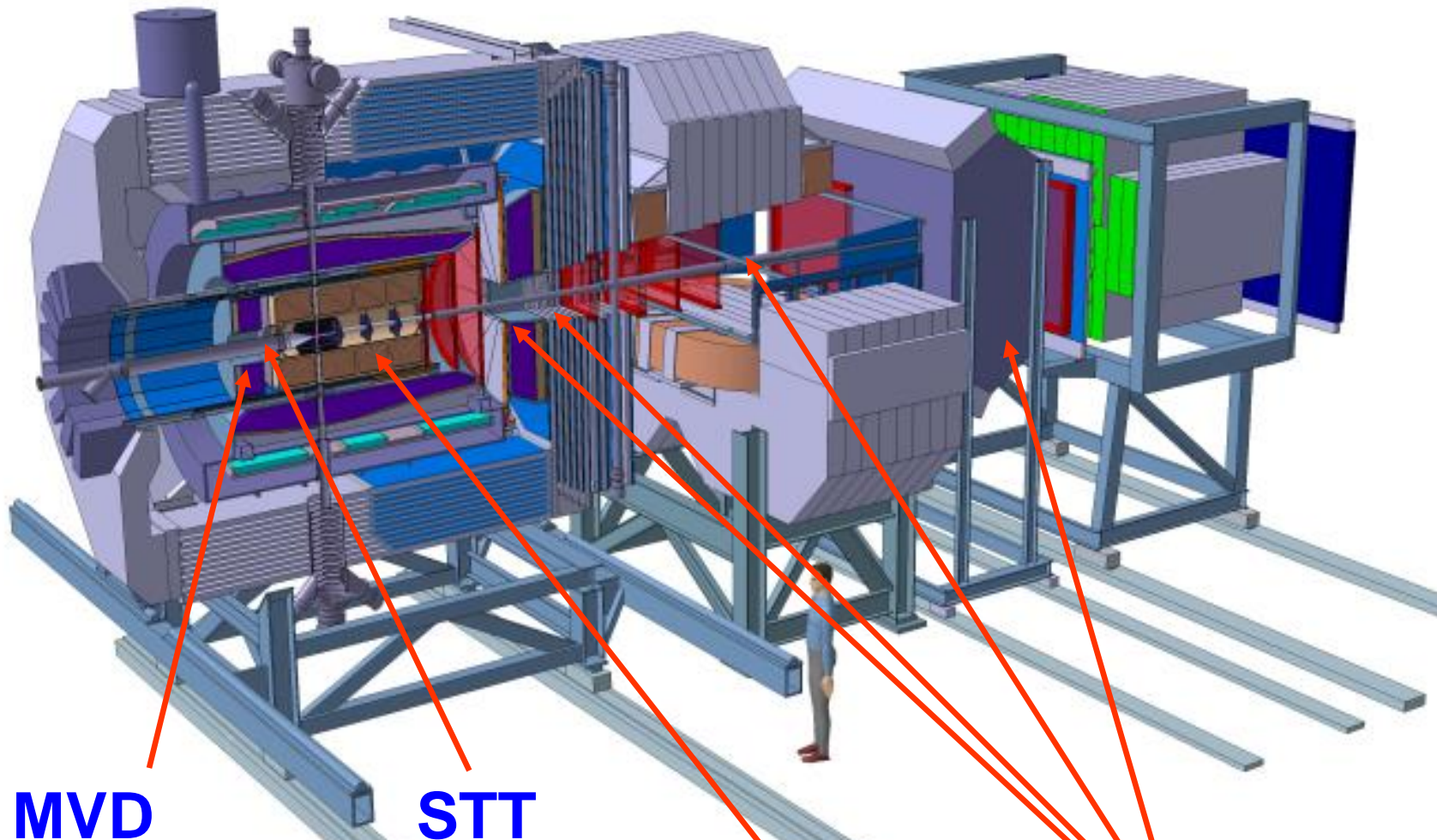
- Cluster Jet Target

- Dense gas jet
- also $\text{D}_2, \text{N}_2, \text{Ne}, \dots$
- Status: $\rho \sim 8 \times 10^{14}$





PANDA spectrometer: Tracking



Silicon MicroVertex

Central Tracker

GEM Detectors

Drift Chambers

Physics Performance Report for PANDA arXiv:0903.3905

PANDA STT TDR arXiv:1205.5441v1 [physics.ins-det]

15-20 Sep 2014

ISHEPP2014



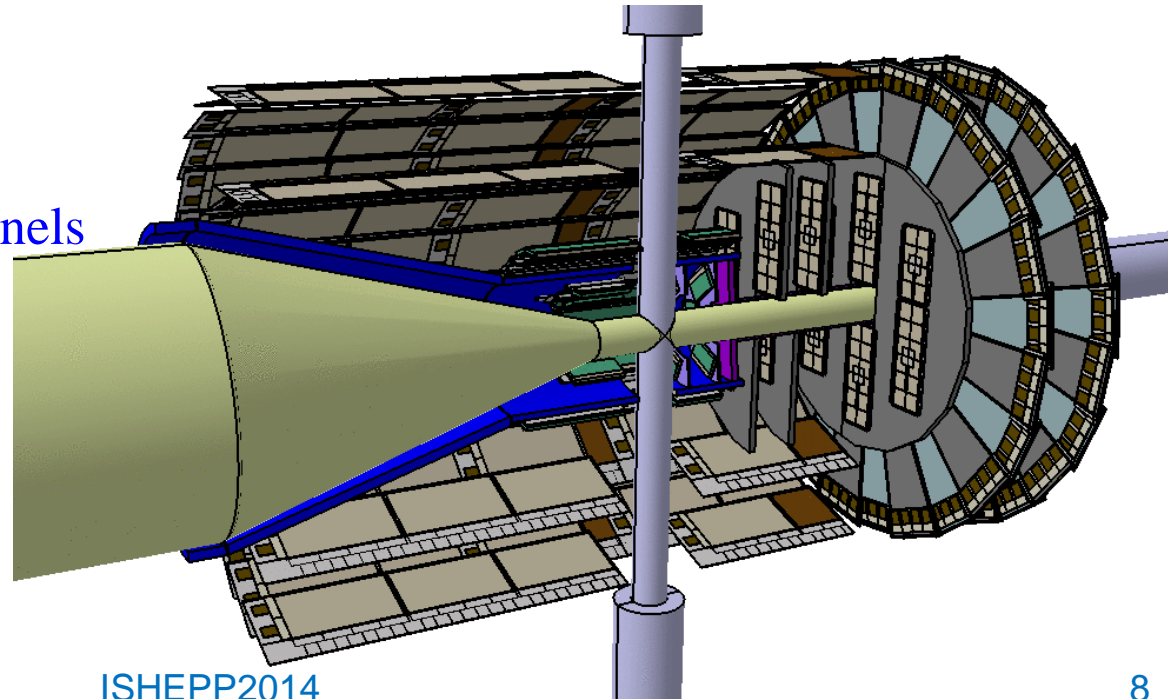
Silicon Microvertex Detector

Micro Vertex Detector

- 4 barrels and 6 disks
- Inner layers:
hybrid pixels ($100 \times 100 \mu\text{m}^2$)
 - 140 module, 12M channels
- Outer layers:
silicon strip detectors
 - double sided strips
 - 400 modules, 200k channels
- Mixed forward disks
- Continuous readout

Requirements

- $c\tau(D^\pm) \sim 312 \mu\text{m}$
 $c\tau(D_s^\pm) \sim 147 \mu\text{m}$
- Vertex resolution $\sim 50 \mu\text{m}$





Central Tracker

- Design figures:

- $\sigma_{r\phi} \sim 150\mu\text{m}$, $\sigma_z \sim 1\text{mm}$
- $\delta p/p \sim 1\div 2\%$ (with MVD)
- Material budget $\sim 2\% X_0$

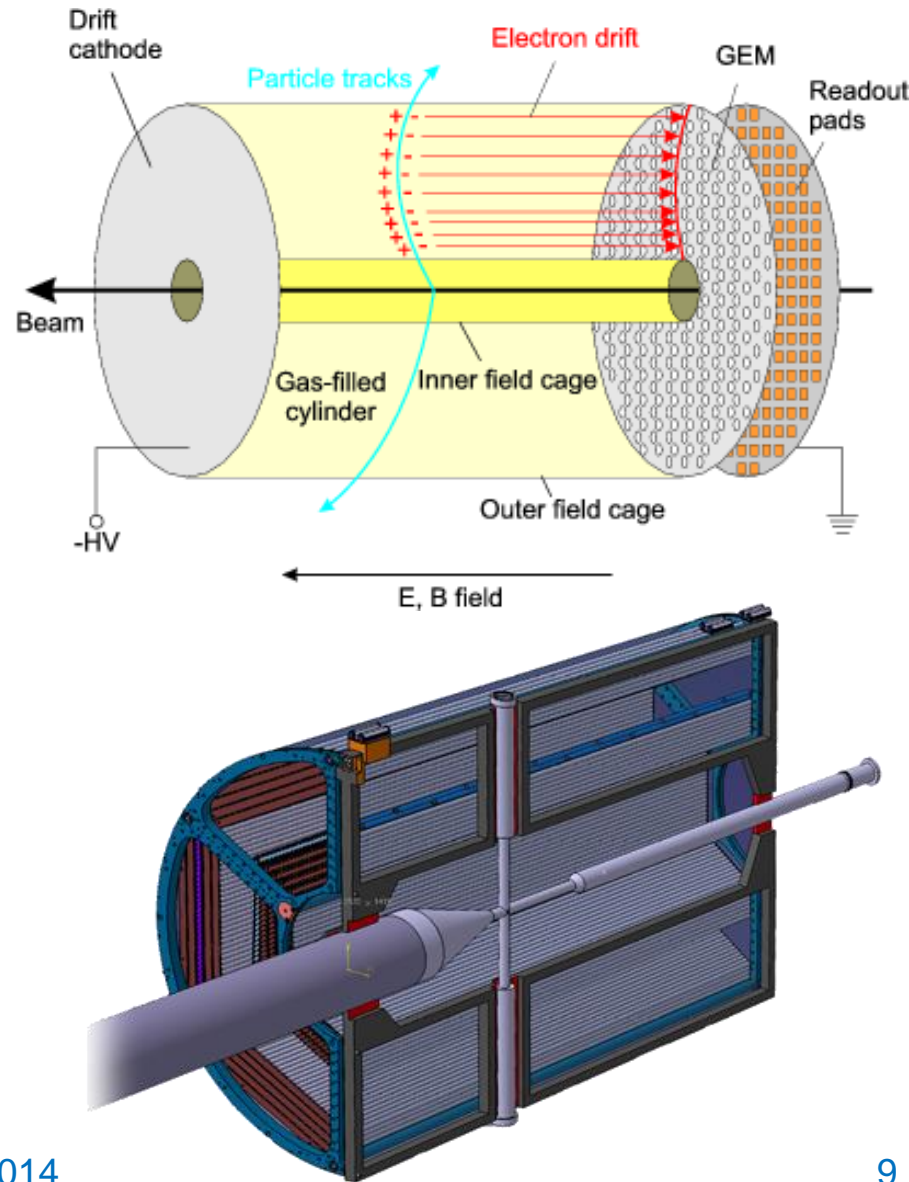
- 2 Alternatives:

- Time Projection Chamber (phased out)

- Continuous sampling
GEMs readout plane
(Ion feedback suppression)
Online tracklet finding

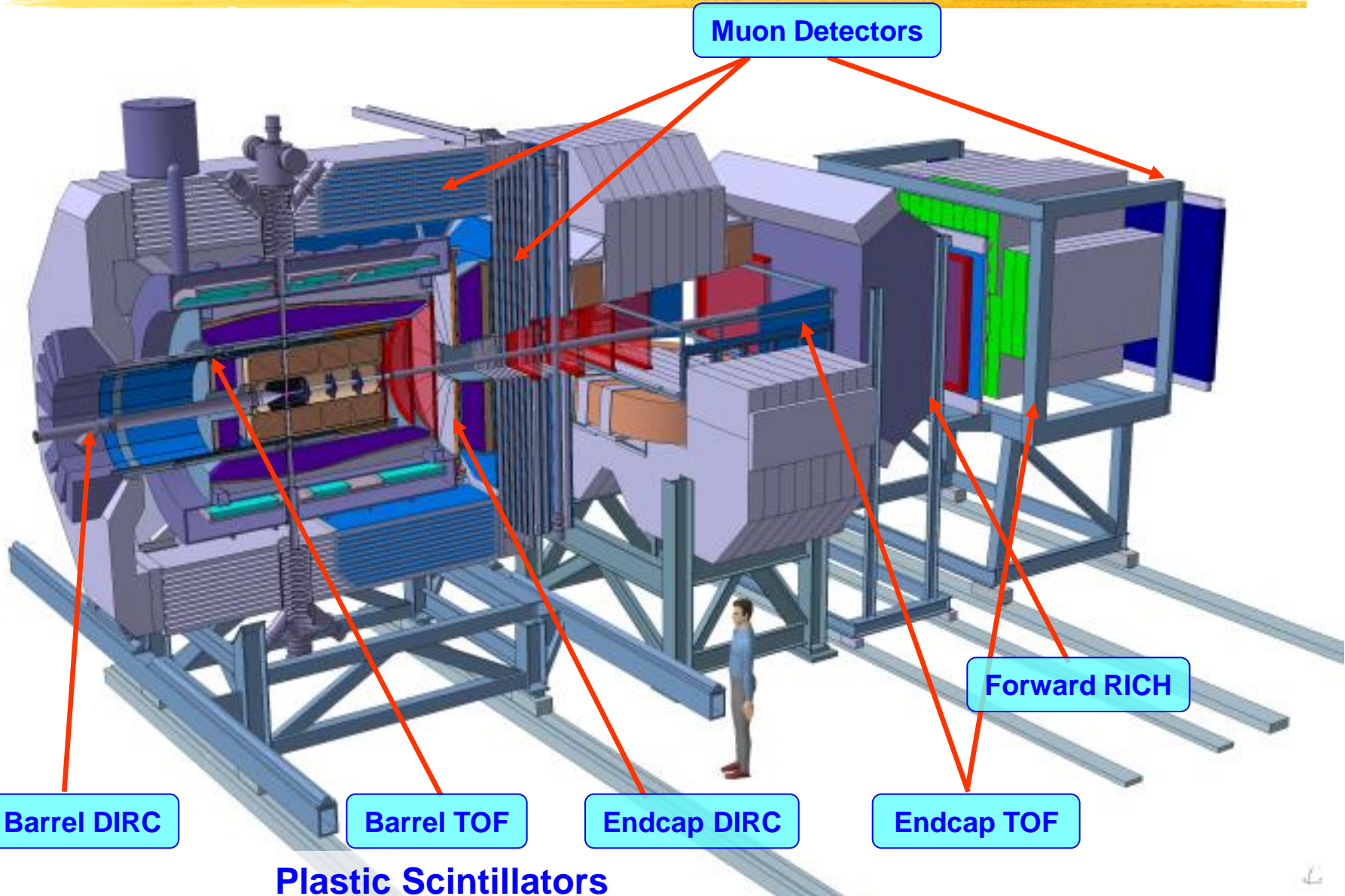
- Straw Tube Tracker (selected!)

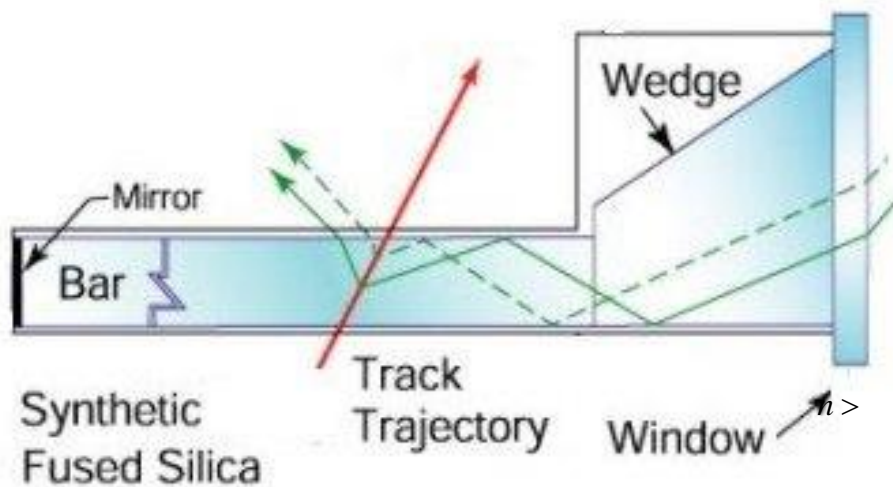
- about 4000 straws
- 27 μm thin mylar tubes, 1 cm \varnothing
- Stability by 1 bar overpressure





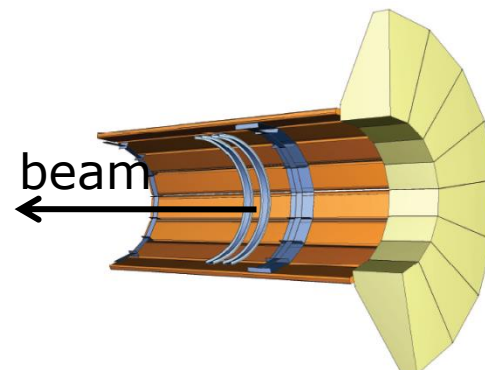
PANDA spectrometer: Particle IDentification



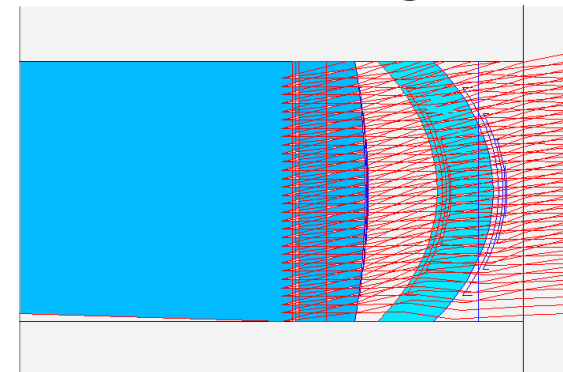


PANDA DIRC

- Lens focussing
- shorter radiator
- no water tank
- compact pixel readout
(CP-PMTs or APDs)



Lens Focussing

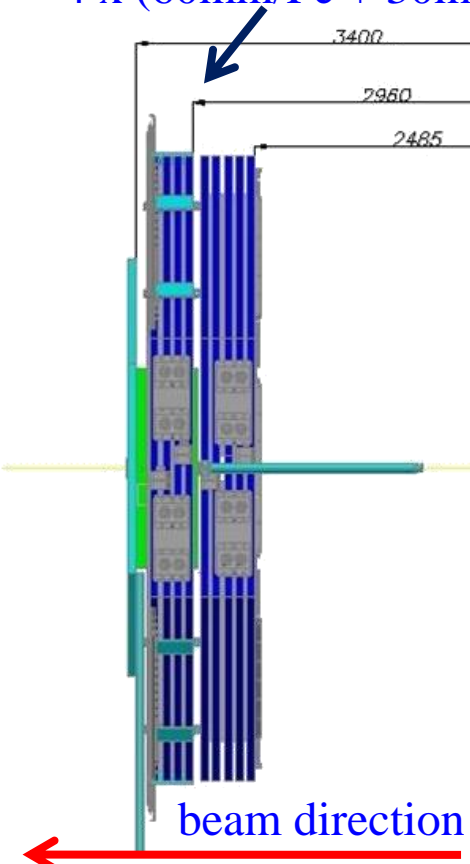




Muon detector

Outside the solenoid
“Muon Filter”, 4 layers

Muon Filter, outside solenoid
4 x (60mm/Fe + 30mm/MDT)



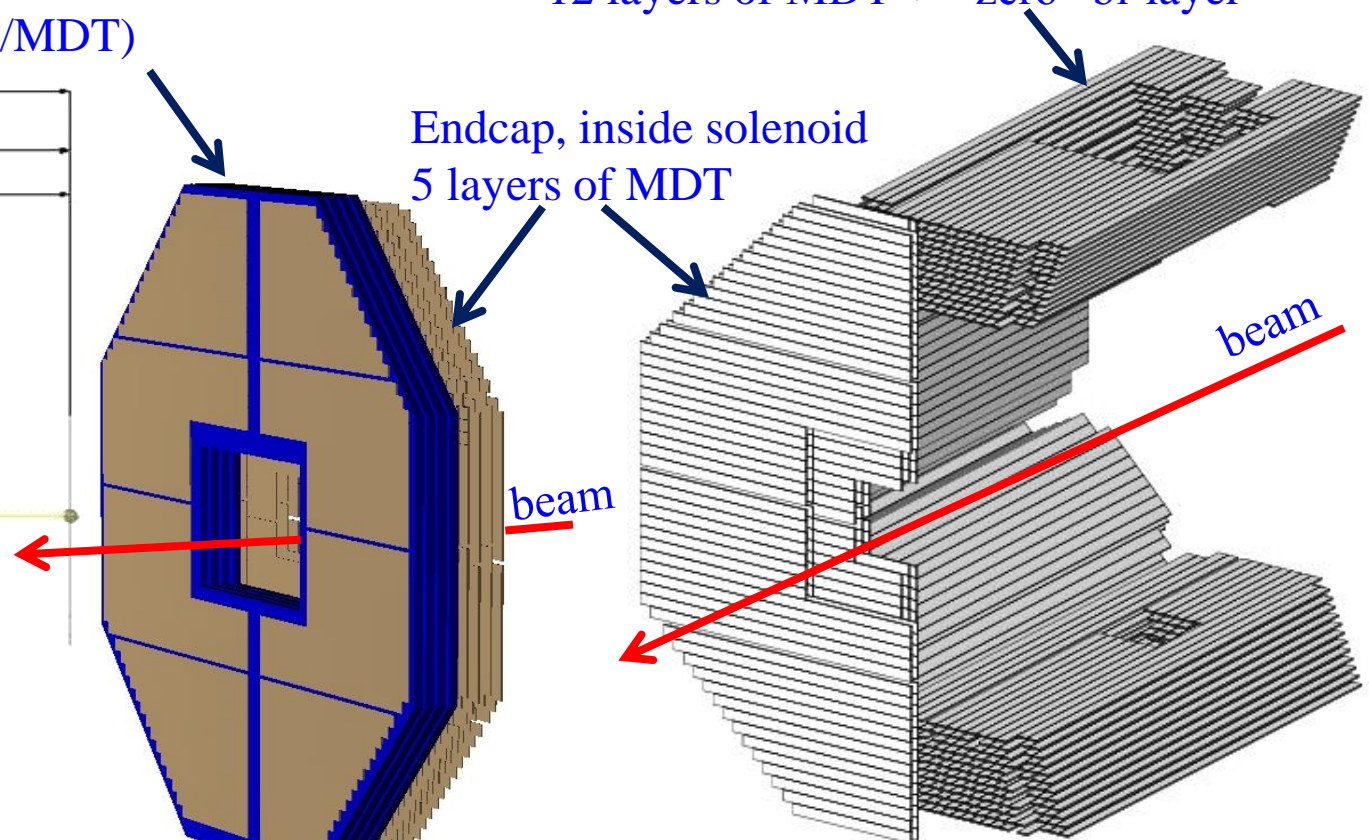
Inside the solenoid

Barrel: 12 layers inside the yoke + 1 bi-layer (“zero” bi-layer) in before iron
Endcap: 5 layers + “zero” bi-layer before iron

Barrel, inside solenoid

12 layers of MDT + “zero” bi-layer

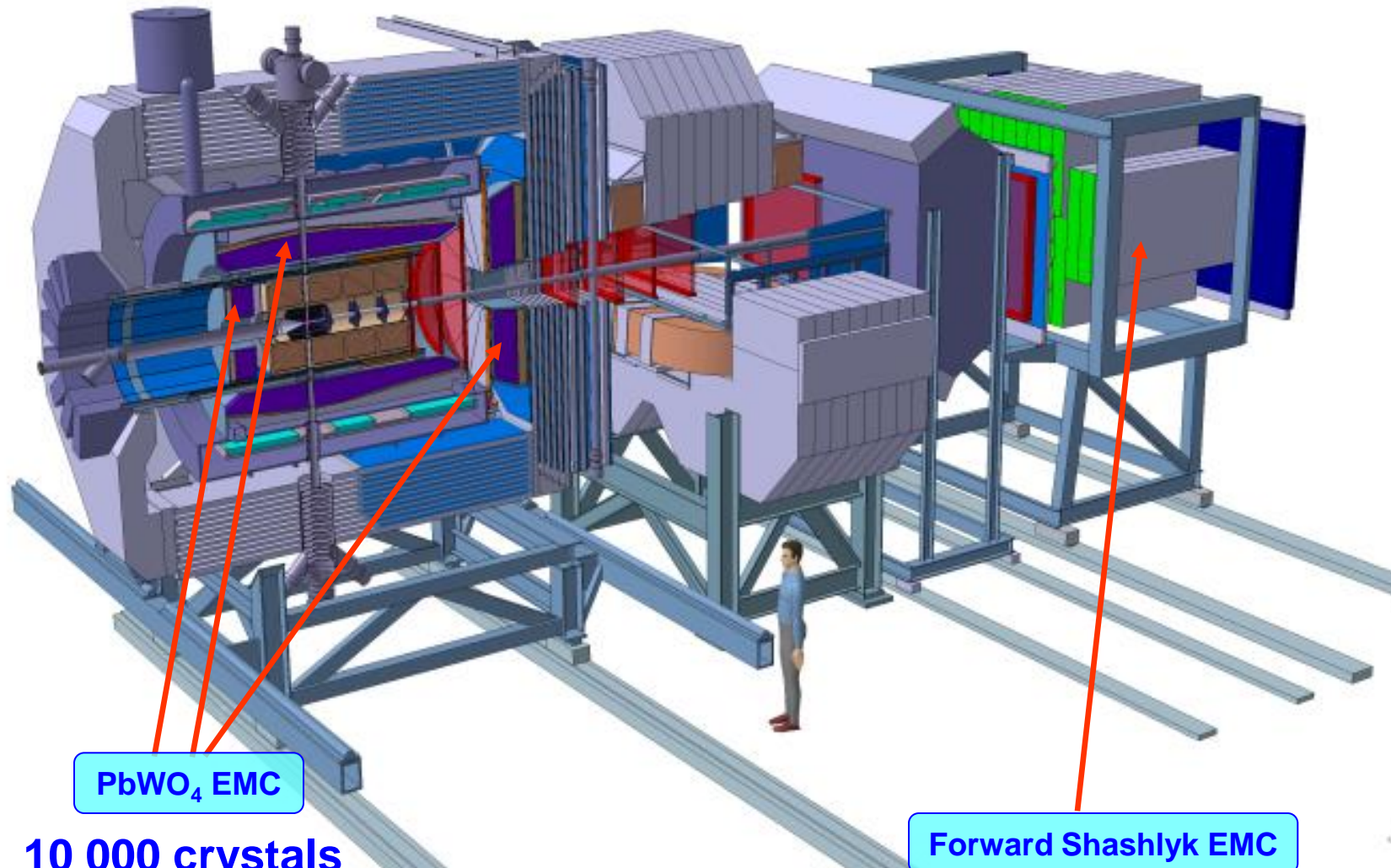
Endcap, inside solenoid
5 layers of MDT



Proportional tubes : anode signal and induction signal on 1 cm strips



PANDA spectrometer: Particle IDentification



10 000 crystals

Forward Shashlyk EMC

Physics Performance Report for PANDA arXiv:0903.3905 [hep-ex]
PANDA EMC TDR arXiv:0810.1216v1 [physics.ins-det]



PANDA PWO Calorimeters

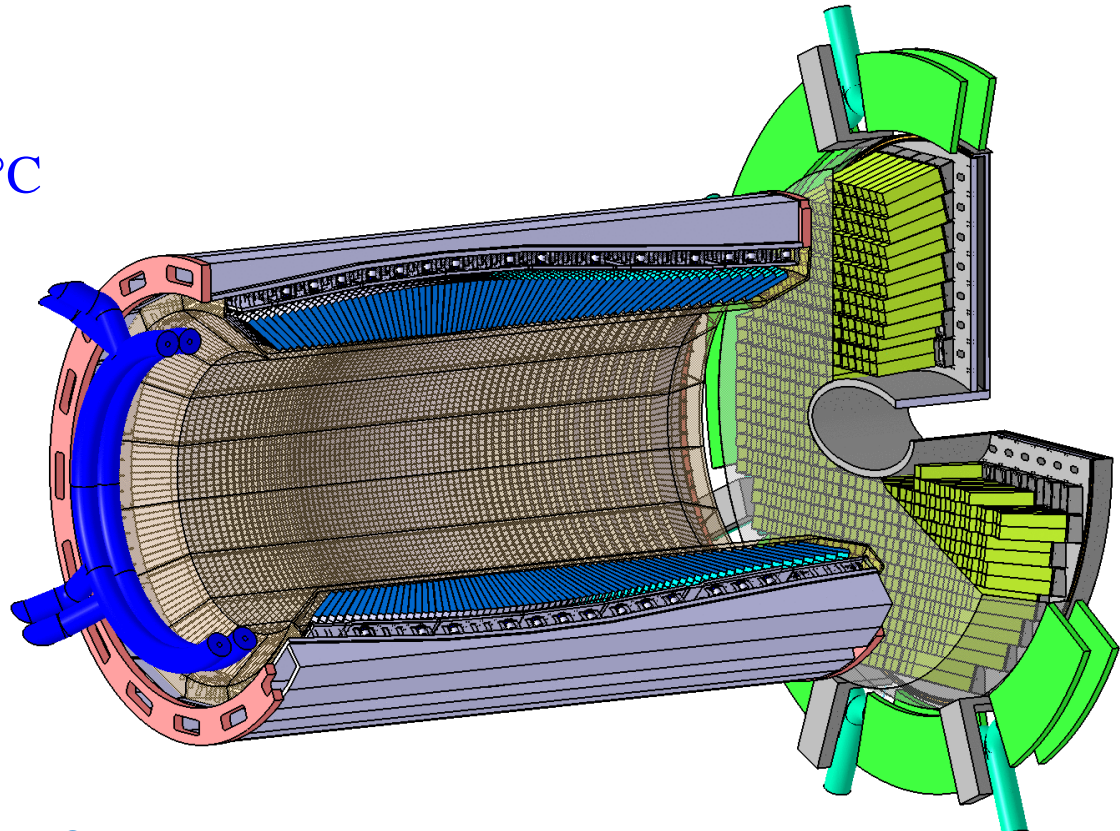
- PWO is dense and fast
- Increase light yield:
 - improved PWO II
 - operation at -25°C
- Challenges:
 - temperature stable to 0.1°C
 - control radiation damage
 - low noise electronics
- Delivery of crystals started

Barrel Calorimeter

- 11000 PWO Crystals
- LAAPD readout, $2 \times 1\text{cm}^2$
- $\sigma(E)/E \sim 1.5\%/\sqrt{E} + \sim 1\%$

Forward Endcap

- 4000 PWO crystals
- High occupancy in center
- LAAPD readout





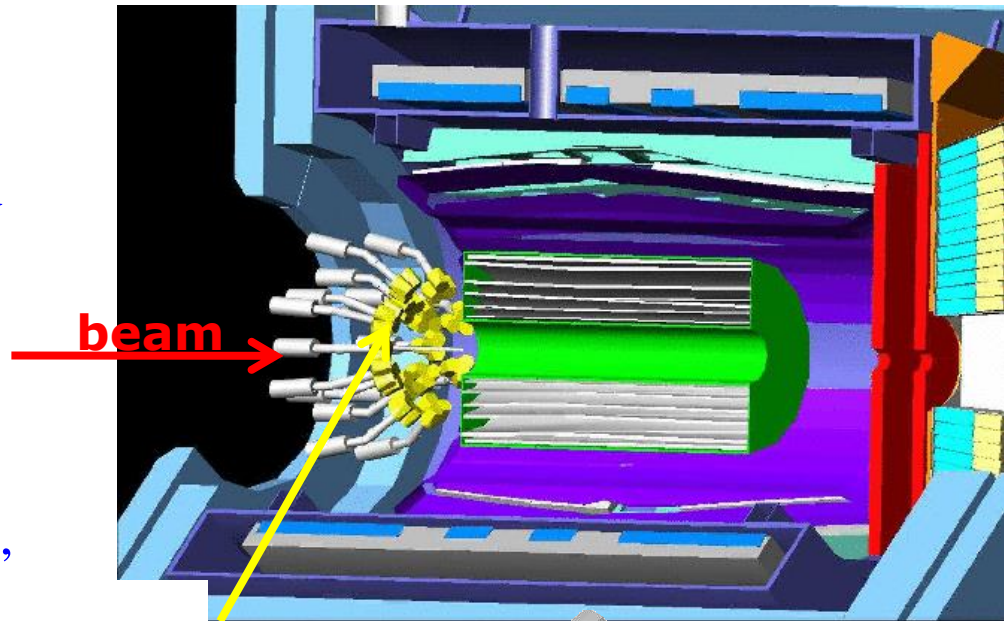
Hypernuclear Detector

Internal C target to produce $\Xi\bar{\Xi}$

Active silicon target to stop the Ξ and detect the hypernuclei decay products

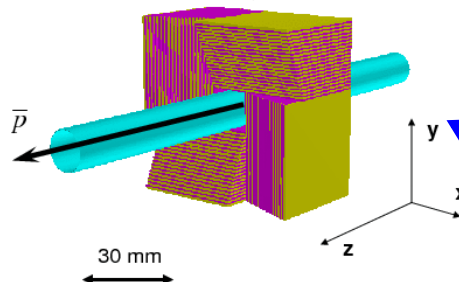
Germanium γ array detector, with 15 clusters of 3 germanium

Foreseen 2 KeV γ energy resolution,
1.3 MeV π energy resolution



Germanium array

**active
target**



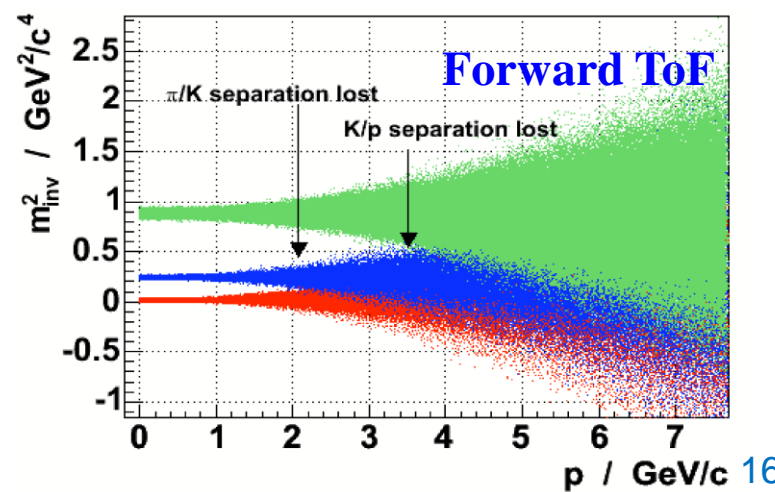
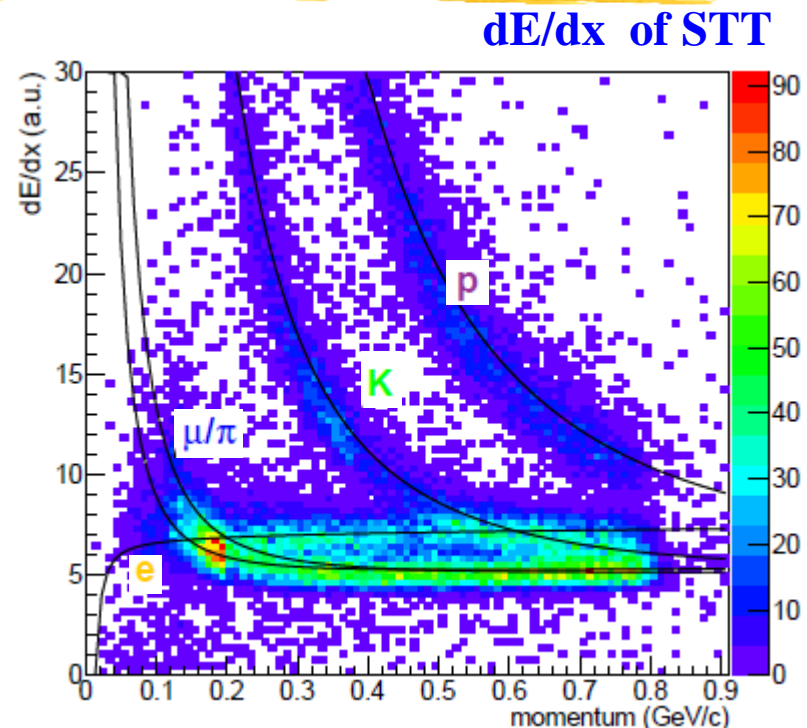


PANDA PID requirements

- Particle identification essential tool
- Momentum range 200 MeV/c – 10 GeV/c
- Different processes for PID needed

PID Processes

- Čerenkov radiation:
Radiators: quartz, aerogel, C_4F_{10}
- Energy loss: $p < 1$ GeV
Good accuracy with TPC,
Stt system dE/dx under study
- Time of flight:
needs a start detector
- Electromagnetic showers:
EMC for e and γ

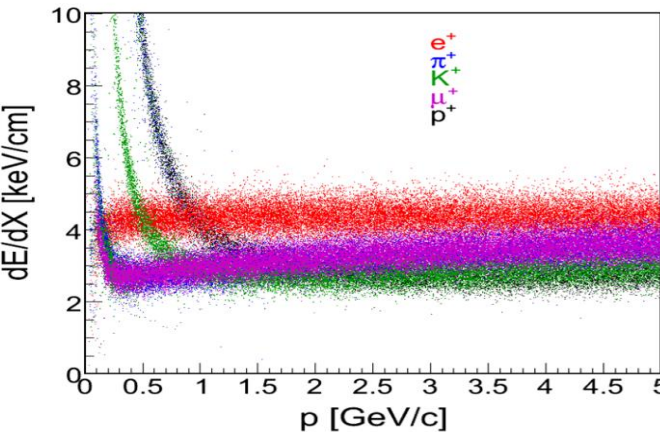




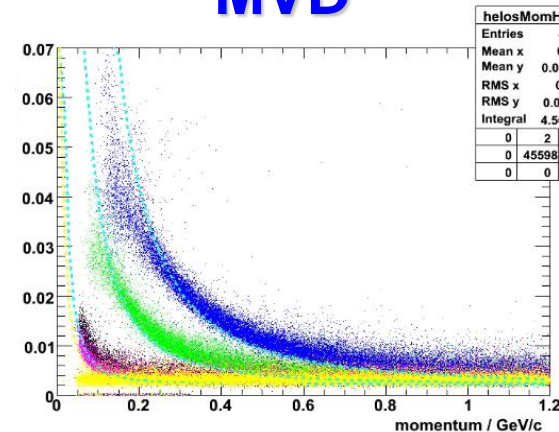
PANDA PID Requirements:

- particle identification essential for PANDA
- momentum range 200 MeV/c – 10 GeV/c
- Extreme high rates $2 \cdot 10^7$ Hz
- good particle separation ($K-\pi$, $e-\pi$)**
 - different detectors needed for PID

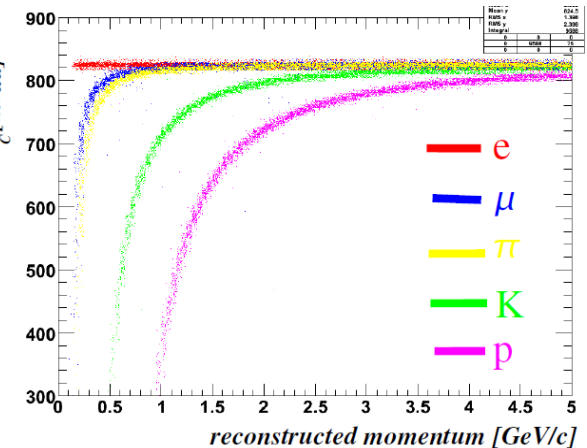
STT



MVD



DIRC





PANDA scientific program

- ## ● baryon/antibaryon production

- ## EM processes:

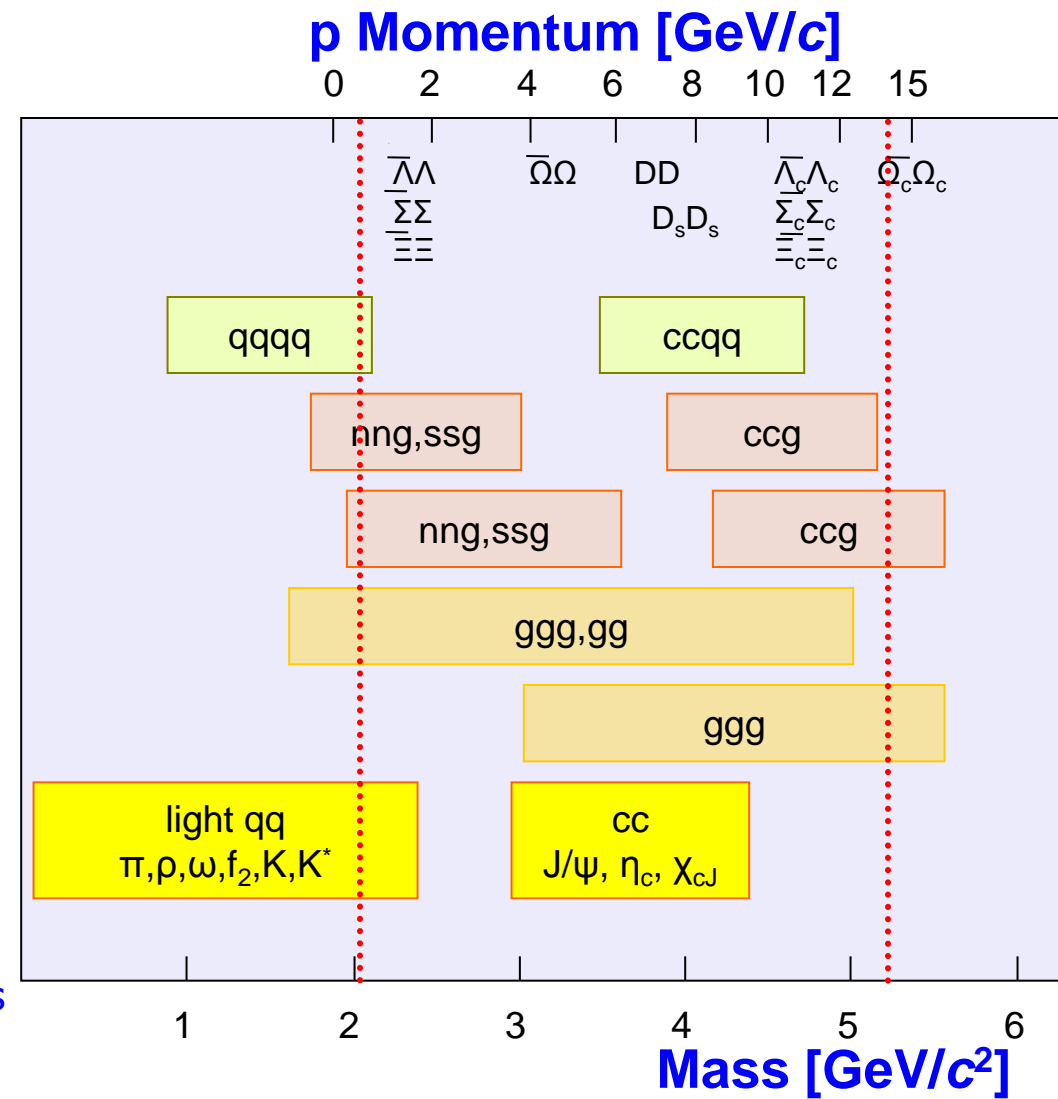
- TL form factors
 - Drell-Yan and TMDS
 - GPDs
 - TDA

- ## ● **strangeness physics**

- hyperatoms
 - S=-2 nuclear system
 - Ξ^- nuclei
 - $\Lambda\Lambda$ hypernuclei

- ## ● meson spectroscopy

- light mesons
 - charmonium
 - exotics states
 - glueballs
 - hybrids
 - molecules/multiquarks
 - open charm



- ## • charm in nuclei



Time-Like EM proton form factors in $\bar{p} + p \rightarrow e^- + e^+$

$$\mathcal{L} = 2 \cdot 10^{32} \text{ cm}^{-2} \text{ s}^{-1} \rightarrow 2 \text{ fb}^{-1} \text{ in } \sim 100 \text{ days}$$

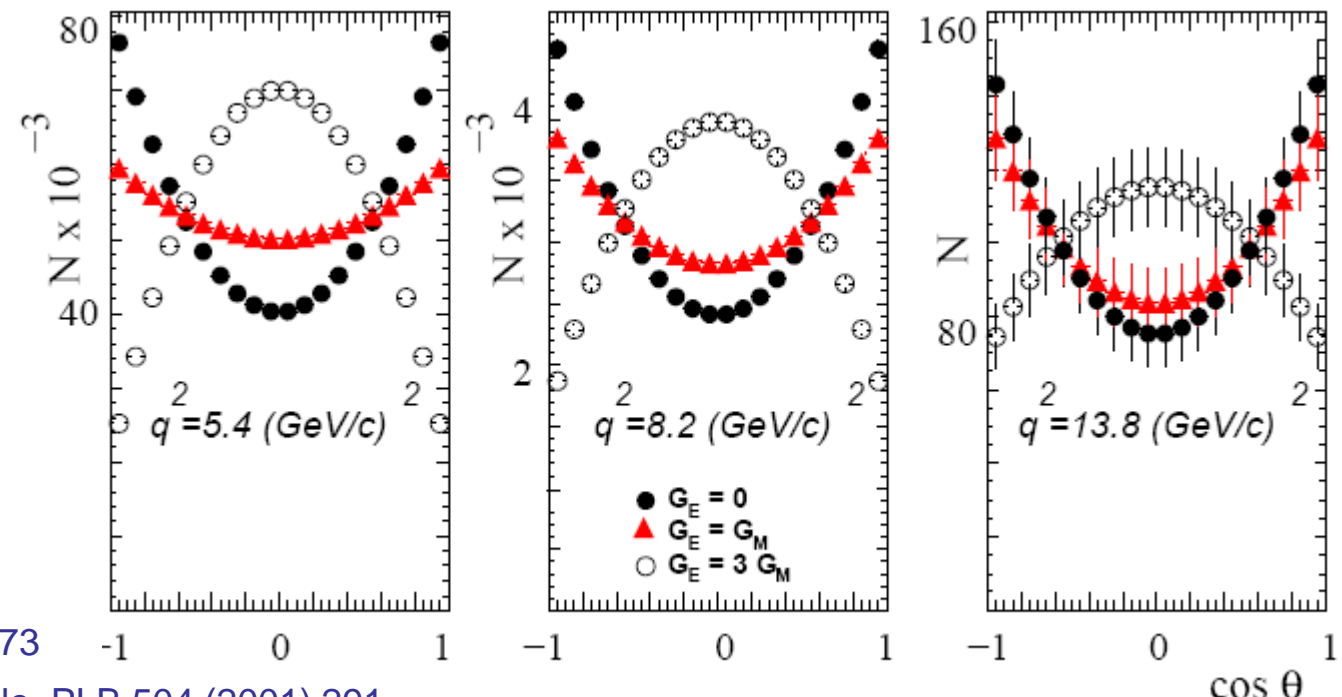
Generator:

- $|G_M| = 22.5 (1 + q^2 / 0.71)^{-2} (1 + q^2 / 3.6)^{-1}$

$$\frac{d\sigma}{d(\cos \theta)} = \frac{\pi \alpha^2}{8m^2 \sqrt{\tau - 1}} [\tau |G_M|^2 (1 + \cos^2 \theta) + |G_E|^2 \sin^2 \theta]$$

- $\mathfrak{R} = |G_E|/|G_M|$

lower sensitivity
@ higher q^2



M. Sudol et al., EPJ A44 (2010) 373

E. Tomasi-Gustafsson, M.P. Rekalo, PLB 504 (2001) 291

15-20 Sep 2014

ISHEPP2014

19



PANDA scenario: expected results



$$\mathcal{L} = 2 \cdot 10^{32} \text{ cm}^{-2} \text{ s}^{-1} \rightarrow 2 \text{ fb}^{-1} \text{ in } \sim 100 \text{ days}$$

$$N(\cos \theta) = \alpha[\tau(1 + \cos^2 \theta) + \mathcal{R}^2 \sin^2 \theta]$$

BABAR:

B. Aubert et al. PRD 73 (2006) 012005

PS170:

G. Bardin et al., NPB 411 (1994) 3

pQCD inspired:

V. A. Matveev et al., LNC 7 (1973) 719

S. J. Brodsky et al., PRL 31 (1973) 1153

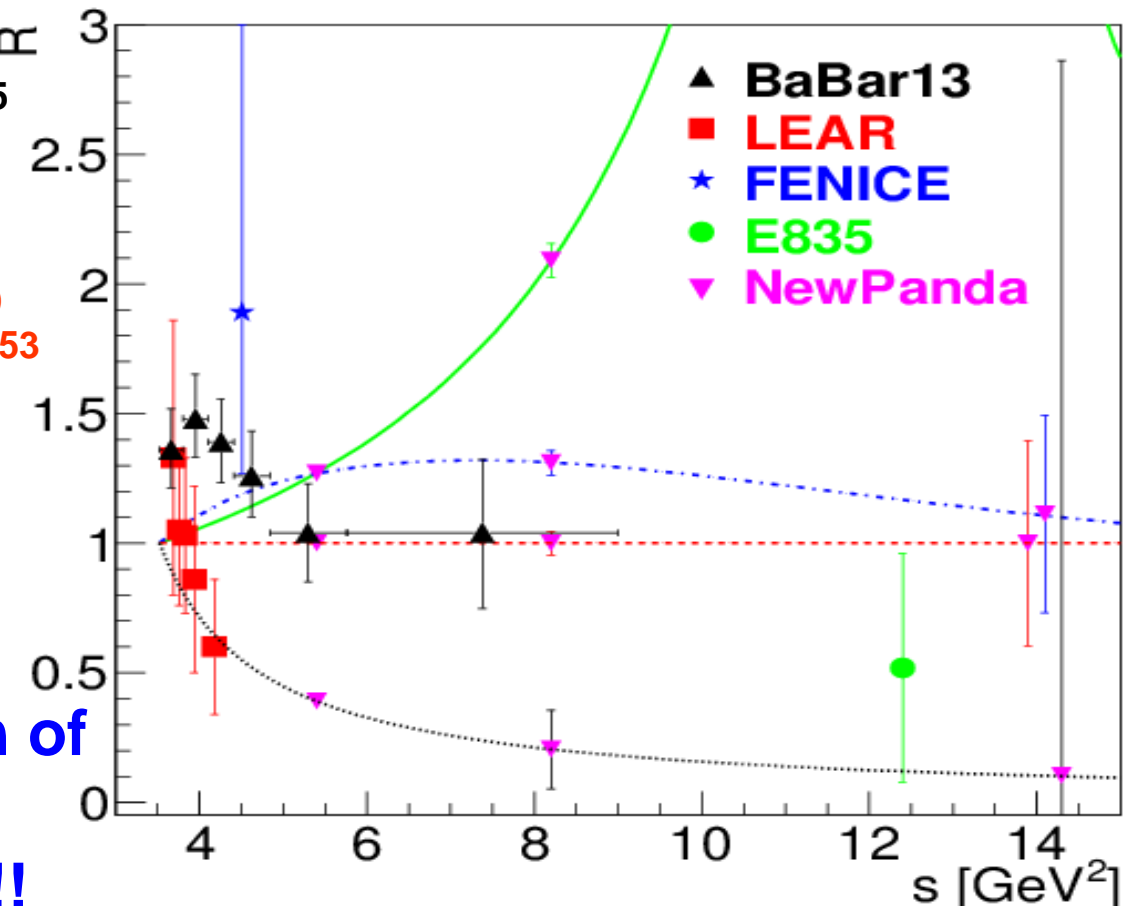
VDM:

F. Iachello, PLB 43 (1973) 191

Extended VDM:

E.L.Lomon, PRC 66 (2002) 045501

E. A. Kuraev et al., PLB 712 (2012) 240



**Individual determination of
|G_E| and |G_M|
up to $q^2 \sim 14 \text{ (GeV/c)}^2$!!**

M. Sudol et al., EPJ A44 (2010) 373

15-20 Sep 2014

A. Dbeysi, PhD Thesis: PANDA unofficial results
ISHEPP2014



PANDA scenario: expected results



$$\mathcal{L} = 2 \cdot 10^{32} \text{ cm}^{-2} \text{ s}^{-1} \rightarrow 2 \text{ fb}^{-1} \text{ in } \sim 100 \text{ days}$$

BABAR:

B. Aubert et al. PRD 73 (2006) 012005

E835:

M. Andreotti et al., PLB 559 (2003) 20

M. Ambrogiani et al., PRD 60 (1999) 032002

Fenice:

A. Antonelli et al., NPB 517 (1998) 3

PS170:

G. Bardin et al., NPB 411 (1994) 3

E760:

T. A. Armstrong et al., PRD 56 (1997) 2509

CLEO:

T. K. Pedlar et al. , PRL 95 (2005) 261803

DM1:

B. Delcourt et al., PLB 86 (1979) 395

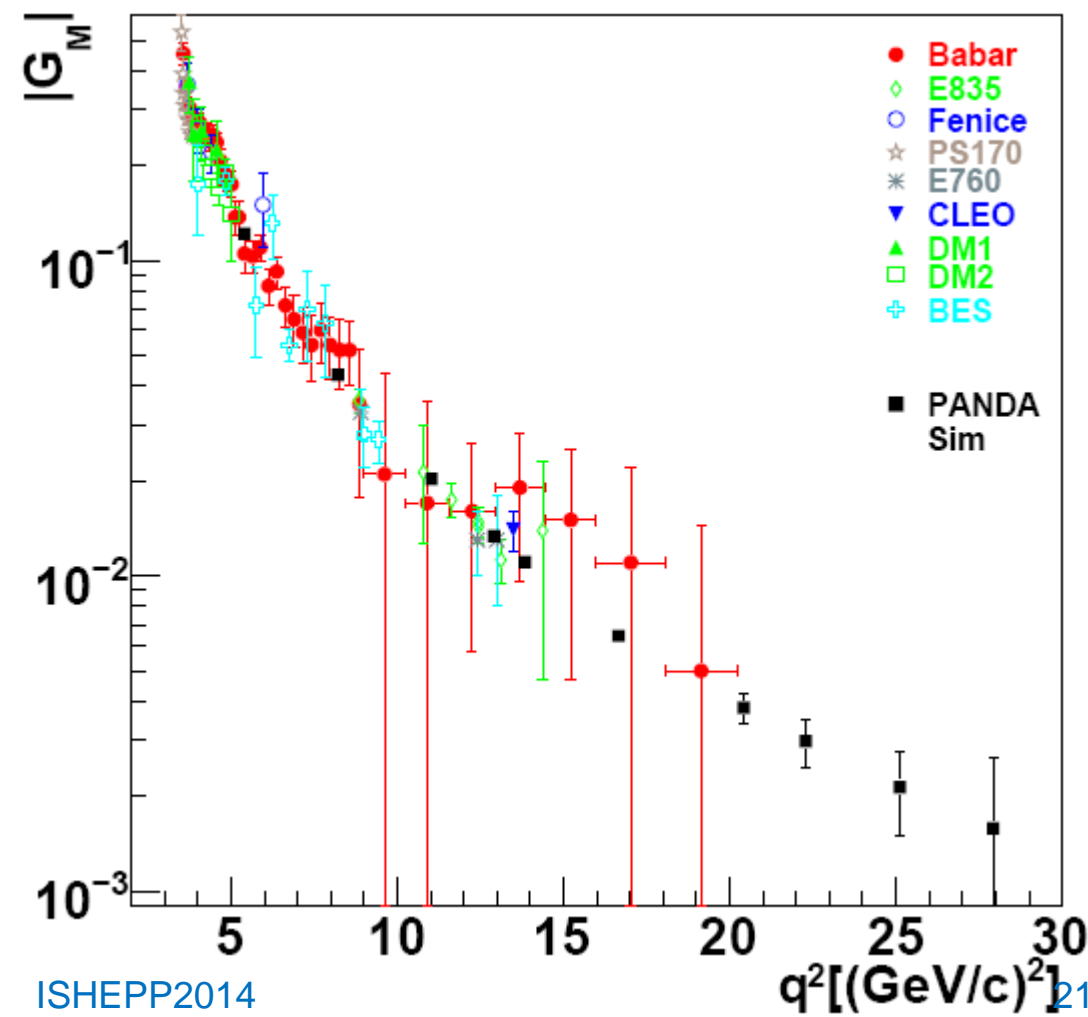
DM2:

D. Bisello et al., NPB 224 (1983) 379

BES:

M. Ablikim et al., PLB 630 (2005) 14

$$\mathcal{R} = 1$$



**Absolute σ accessible
up to $q^2 \sim 28 (\text{GeV}/c)^2$**

M. Sudol et al., EPJ A44 (2010) 373

15-20 Sep 2014

ISHEPP2014

21



PANDA scenario: asymptotic behaviours



$$\mathcal{L} = 2 \cdot 10^{32} \text{ cm}^{-2} \text{ s}^{-1} \rightarrow 2 \text{ fb}^{-1} \text{ in } \sim 100 \text{ days}$$

BABAR:

B. Aubert et al. PRD 73 (2006) 012005

E835:

M. Andreotti et al., PLB 559 (2003) 20

M. Ambrogiani et al., PRD 60 (1999) 032002

Fenice:

A. Antonelli et al., NPB 517 (1998) 3

PS170:

G. Bardin et al., NPB 411 (1994) 3

E760:

T. A. Armstrong et al., PRD 56 (1997) 2509

CLEO:

T. K. Pedlar et al. , PRL 95 (2005) 261803

DM1:

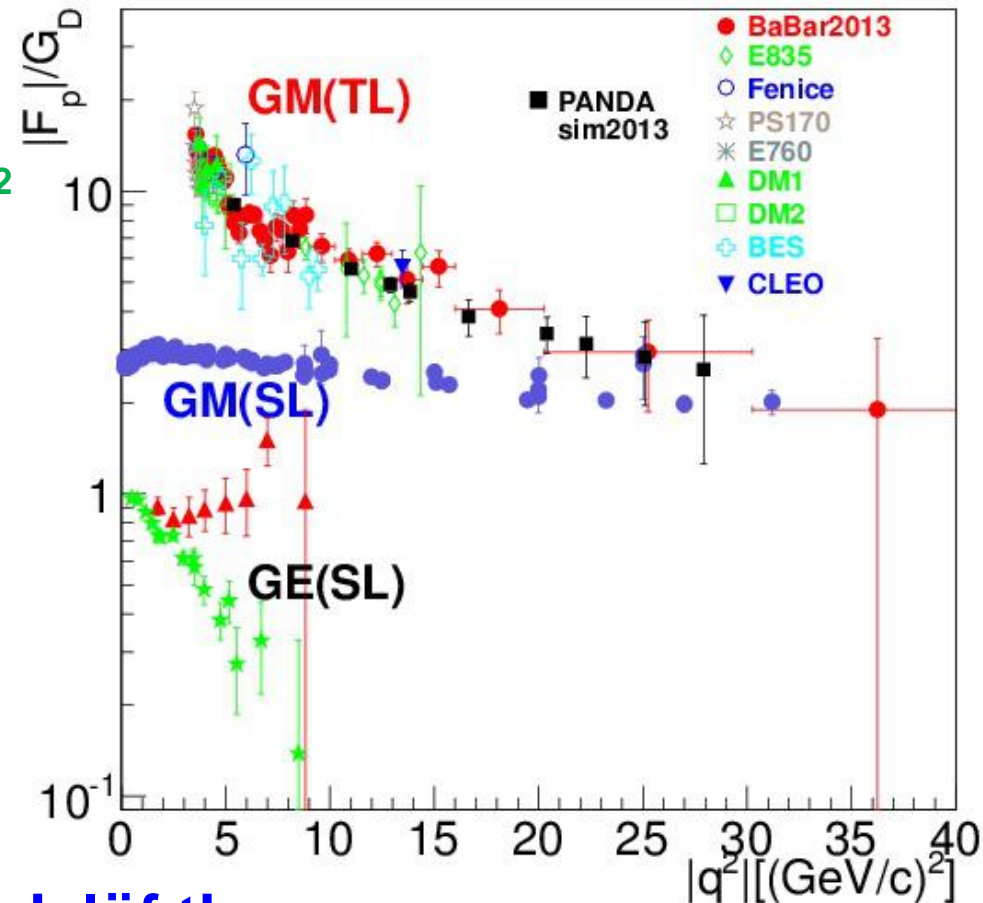
B. Delcourt et al., PLB 86 (1979) 395

DM2:

D. Bisello et al., NPB 224 (1983) 379

BES:

M. Ablikim et al., PLB 630 (2005) 14



Probing the Phragmèn-Lindelöf theorem:

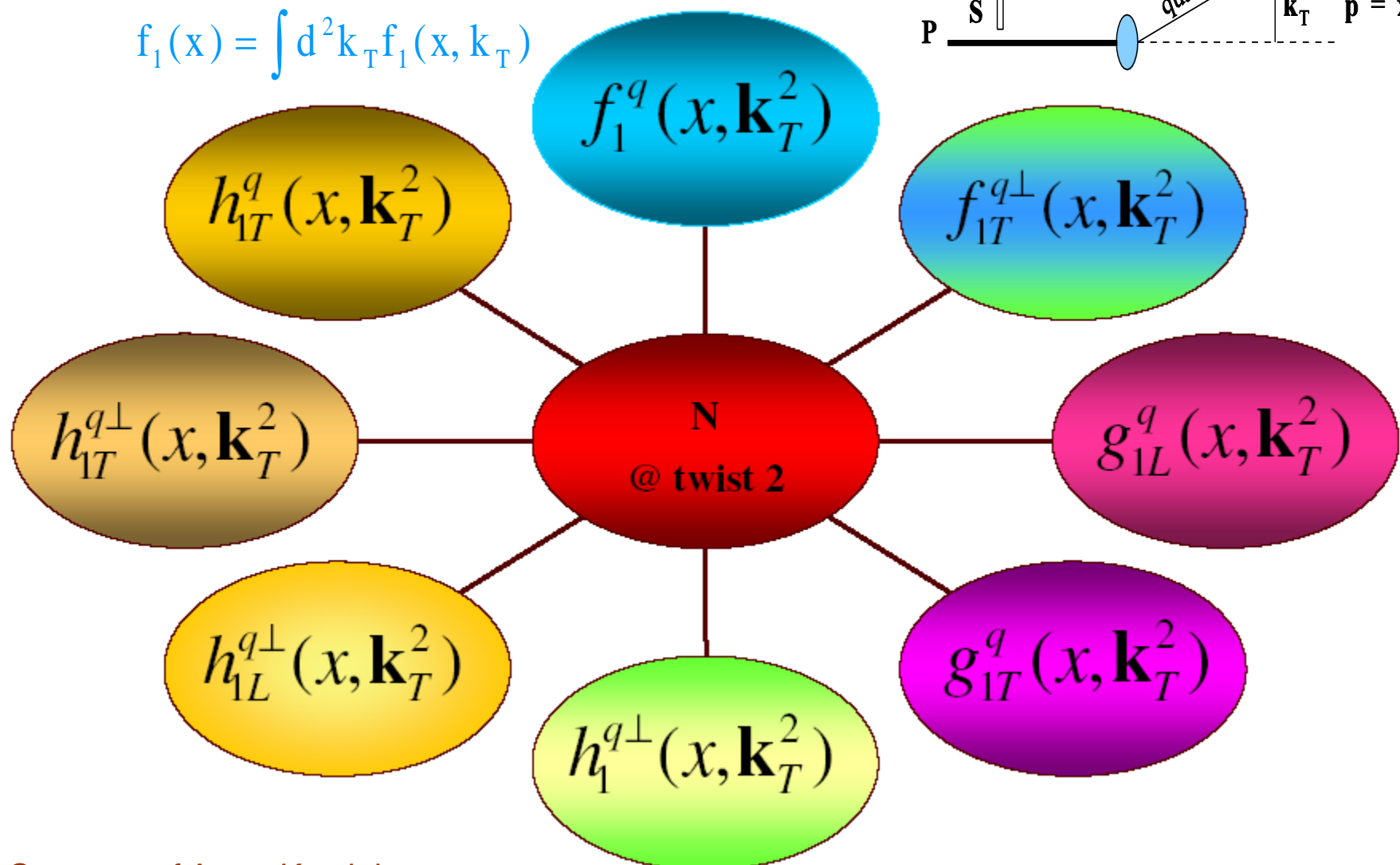
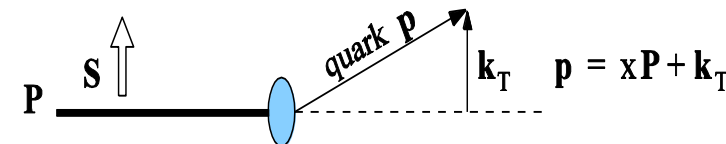
$$\lim_{q^2 \rightarrow -\infty} F^{(SL)}(q^2) = \lim_{q^2 \rightarrow \infty} F^{(TL)}(q^2) \quad Im F_i(q^2) \rightarrow 0, \quad q^2 \rightarrow \infty$$



TMD: κ_T -dependent Parton Distributions

Twist-2 PDFs:

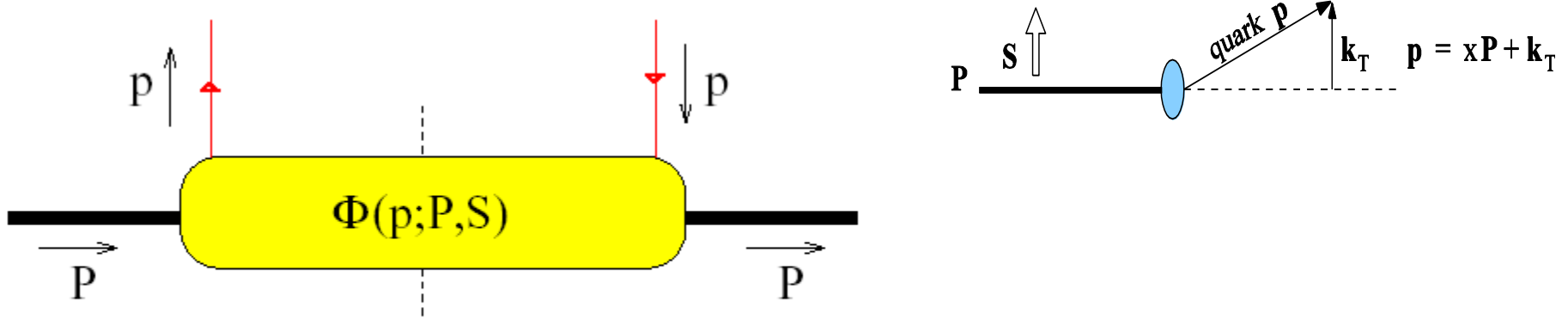
$$f_1(x) = \int d^2 k_T f_1(x, k_T)$$





TMD: κ_T -dependent Parton Distributions

Leading-twist correlator depends on
five more distribution functions:



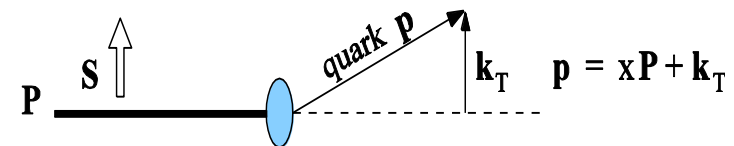
$$\begin{aligned} \Phi(x_a, \mathbf{k}_{\perp a}) = & \frac{1}{2} \left[f_1 h_+ + f_{1T}^{\perp} \frac{\epsilon_{\mu\nu\rho\sigma} \gamma^\mu n_+^\nu k_{\perp a}^\rho (P_T^A)^\sigma}{M} + \left(P_L^A g_{1L} + \frac{\mathbf{k}_{\perp a} \cdot \mathbf{P}_T^A}{M} g_{1T}^{\perp} \right) \gamma^5 h_+ \right. \\ & + h_{1T} i \sigma_{\mu\nu} \gamma^5 n_+^\mu (P_T^A)^\nu + \left(P_L^A h_{1L}^{\perp} + \frac{\mathbf{k}_{\perp a} \cdot \mathbf{P}_T^A}{M} h_{1T}^{\perp} \right) \frac{i \sigma_{\mu\nu} \gamma^5 n_+^\mu k_{\perp a}^\nu}{M} \\ & \left. + h_1^{\perp} \frac{\sigma_{\mu\nu} k_{\perp a}^\mu n_+^\nu}{M} \right]. \end{aligned}$$



TMD: κ_T -dependent Parton Distributions

Twist-2 PDFs

$$f_1(x) = \int d^2 k_T f_1(x, k_T)$$



$$f_1 =$$

$$g_{1L} =$$

$$g_{1T} =$$

$$h_{1T} =$$

$$f_{1T}^\perp =$$

$$h_1^\perp =$$

$$h_{1L}^\perp =$$

Transversity

Sivers

Boer-Mulders

	Distribution functions		Chirality	
			even	odd
Twist-2	U	f_1	h_1^\perp	
	L	g_1	h_{1L}^\perp	
	T	f_{1T}^\perp, g_{1T}	h_1, h_{1T}^\perp	

$$h_{1T}^\perp =$$



Drell-Yan Di-Lepton Production — $\bar{p}p \rightarrow \ell^+ \ell^- X$

Why Drell Yan?

Asymmetries depend on PD only (SIDIS→convolution with QFF)

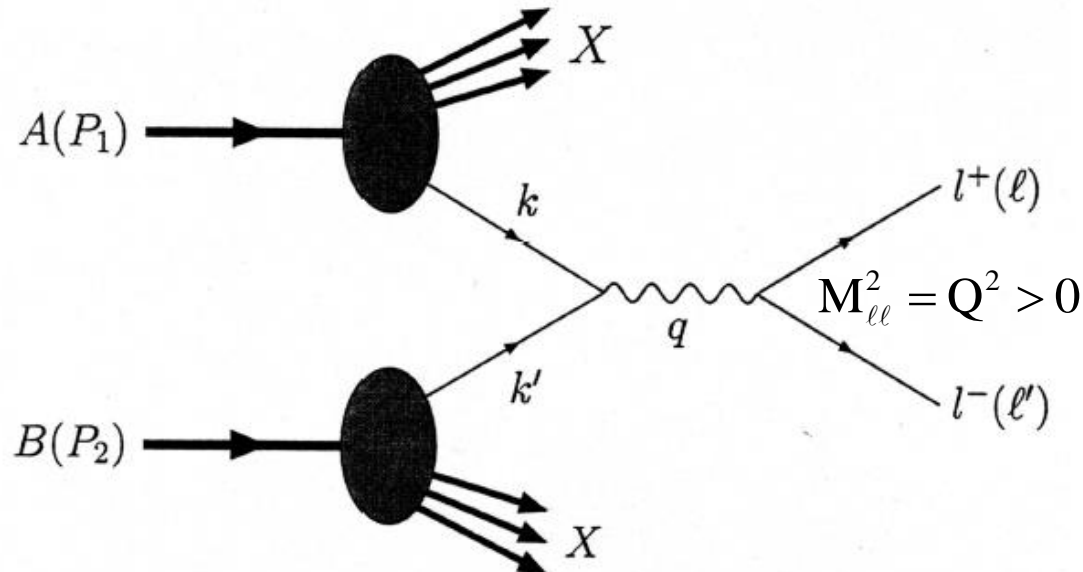
3 planes: plane \perp to polarisation vectors

$p - \gamma^*$ plane
 $\ell^+ \ell^- \gamma^*$ plane

→ plenty of (single) spin effects

Why \bar{p} ?

Each valence quark can contribute to the diagram



Kinematics

$$x_1 = \frac{\mathbf{M}^2}{2\mathbf{P}_1 \bullet \mathbf{q}} \quad x_2 = \frac{\mathbf{M}^2}{2\mathbf{P}_2 \bullet \mathbf{q}}$$

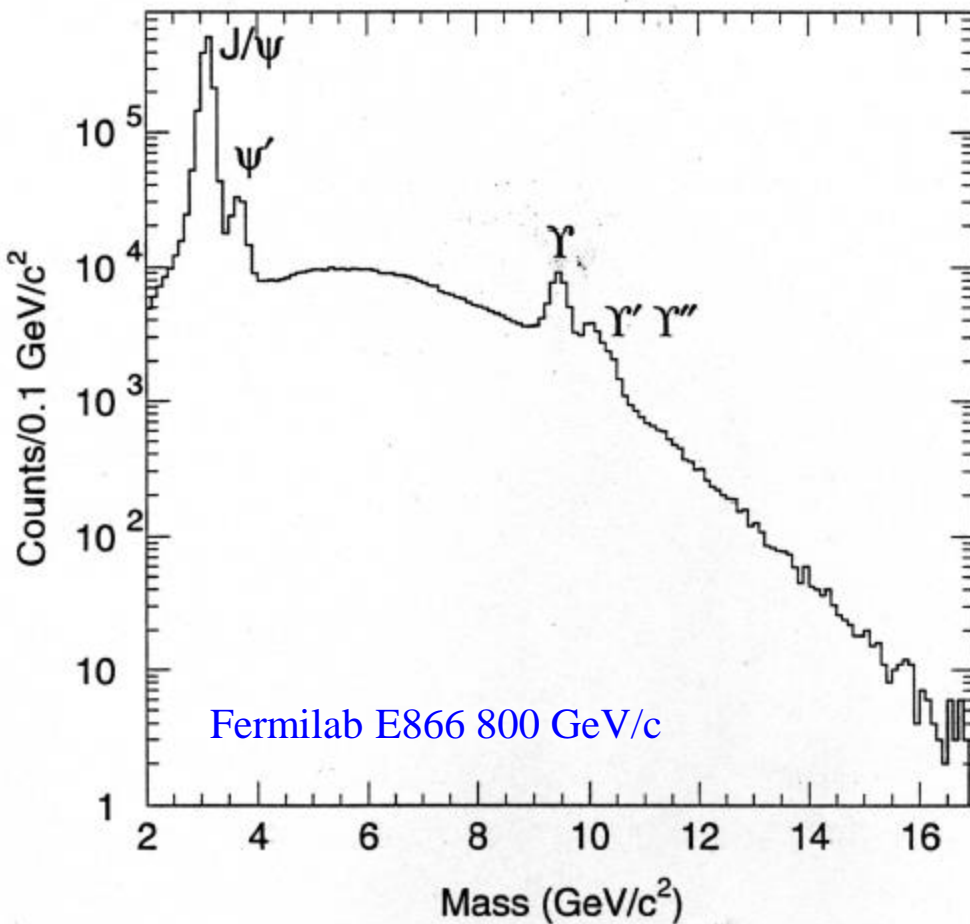
$$\mathbf{X}_F = \mathbf{X}_1 - \mathbf{X}_2$$

$$\tau = x_1 x_2 = \frac{\mathbf{M}^2}{s}$$



Drell-Yan Di-Lepton Production — $\bar{p}p \rightarrow \ell^+ \ell^- X$

$$\frac{d^2\sigma}{dM^2 dx_F} = \frac{4\alpha^2 \pi}{9M^2 s} \frac{1}{x_1 + x_2} \sum_a e_a^2 \left[f^a(x_1) f^{\bar{a}}(x_2) + f^{\bar{a}}(x_1) f^a(x_2) \right]$$



Scaling:

$$\frac{d^2\sigma}{d\sqrt{\tau} dx_F} \propto \frac{1}{s}$$

Full x_1, x_2 range $\Rightarrow \tau \in [0,1]$

Kinematics

$$x_1 = \frac{M^2}{2P_1 \bullet q} \quad x_2 = \frac{M^2}{2P_2 \bullet q}$$

$$X_F = X_1 - X_2$$

$$\tau = x_1 x_2 = \frac{M^2}{s}$$



Experimental Asymmetries @ PANDA — $\bar{p} p^{(\uparrow)} \rightarrow \mu^+ \mu^- X$

Unpolarised:

$$\frac{d\sigma^0}{d\Omega dx_1 dx_2 d\mathbf{k}_T} = \frac{\alpha^2}{12Q^2} \sum_a e_a^2 \left\{ (1 + \cos^2 \theta) \mathcal{F} \left[\bar{f}_1^a f_1^a \right] + \sin^2 \theta \cos 2\phi \mathcal{F} \left[(2\mathbf{h} \square \mathbf{p}_{1T} \mathbf{h} \square \mathbf{p}_{2T} - \mathbf{p}_{1T} \square \mathbf{p}_{2T}) \frac{\bar{h}_1^{\perp a} h_1^{\perp a}}{M_1 M_2} \right] \right\}$$

$$\mathcal{F} \left[\bar{f}_1^a f_1^a \right] \equiv \int d\mathbf{p}_{1T} d\mathbf{p}_{2T} \delta(\mathbf{p}_{1T} + \mathbf{p}_{2T} - \mathbf{k}_T) \left[\bar{f}_1^a(x_1, \mathbf{p}_{1T}) f_1^a(x_2, \mathbf{p}_{2T}) + (1 \leftrightarrow 2) \right]$$

Single Spin:

$$\frac{d\Delta\sigma \uparrow}{d\Omega dx_1 dx_2 d\mathbf{k}_T} = \frac{\alpha^2}{12sQ^2} \sum_a e_a^2 |\mathbf{S}_{2T}| \left\{ (1 + \cos^2 \theta) \sin(\phi - \phi_{S_2}) \mathcal{F} \left[\mathbf{h} \square \mathbf{p}_{2T} \frac{\bar{f}_1^a f_{1T}^{\perp a}}{M_2} \right] + \right.$$

$$- \sin^2 \theta \sin(\phi + \phi_{S_2}) \mathcal{F} \left[\mathbf{h} \square \mathbf{p}_{1T} \frac{\bar{h}_1^{\perp a} h_{1T}^a}{M_1} \right]$$

$$- \sin^2 \theta \sin(3\phi - \phi_{S_2}) \mathcal{F} \left[\left(4\mathbf{h} \square \mathbf{p}_{1T} (\mathbf{h} \square \mathbf{p}_{2T})^2 - 2\mathbf{h} \square \mathbf{p}_{2T} \mathbf{p}_{1T} \square \mathbf{p}_{2T} - \mathbf{h} \square \mathbf{p}_{1T} \mathbf{p}_{2T}^2 \right) \frac{\bar{h}_1^{\perp a} h_{1T}^{\perp a}}{2M_1 M_2} \right]$$

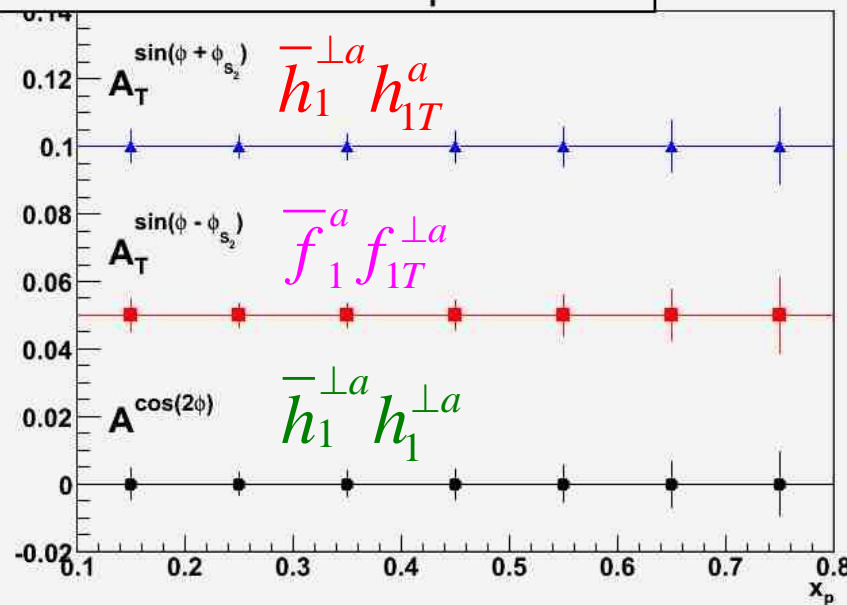


Experimental Asymmetries @ PANDA — \bar{p} p^(↑) → $\mu^+ \mu^- X$

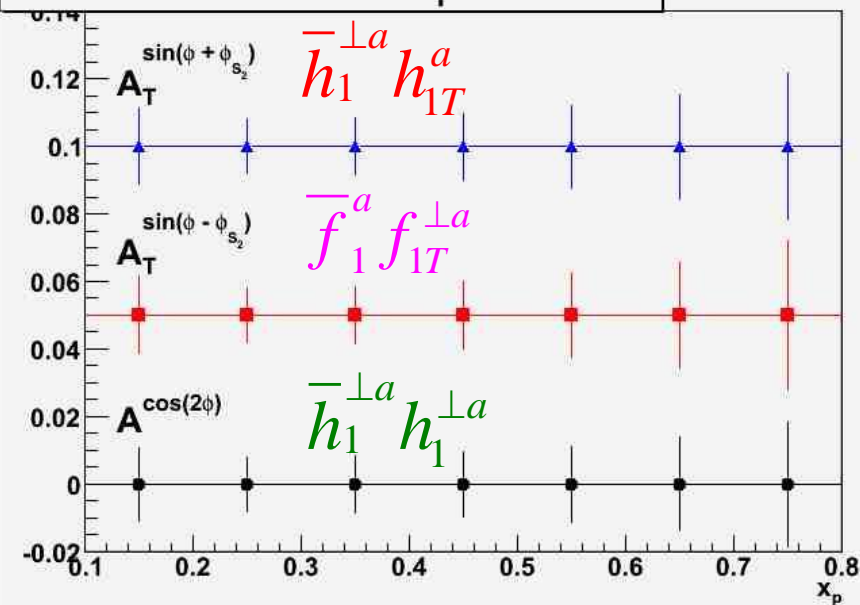
480K ev^[1] with $E_{\bar{p}} = 15$ GeV on fixed target, $1.5 < M_{\mu\mu} < 2.5$ GeV/c²

$$\text{Eff R}_{\text{DY-}\mu\mu}^{[2]} \left(1.5 < M_{\mu\mu} < 2.5 \text{ GeV/c}^2 \right) = 0.16 \text{ s}^{-1} \times \frac{1}{2} = 0.08 \text{ s}^{-1} \square 200 \text{K Ev month}^{-1}$$

Expected errors ($1 < q_T < 2$ GeV/c)



Expected errors ($2 < q_T < 3$ GeV/c)



$s \sim 30$ GeV²

[1] A. Bianconi and M. Radici, Phys. Rev. D71 (2005) 074014

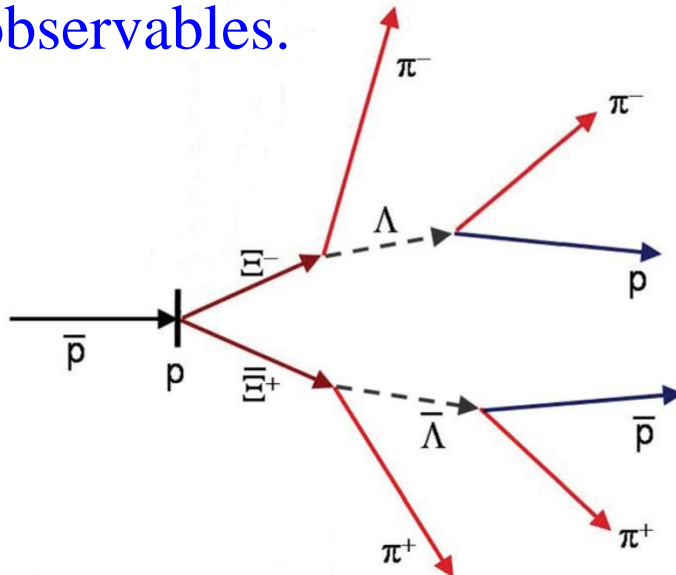
[2] Physics Performance Report for PANDA, arXiv: 0903.3905



QCD dynamics

The experimental data set available is far from being complete. All strange hyperons and single charmed hyperons are energetically accessible in $p\bar{p}$ collisions at PANDA.

In PANDA $p\bar{p} \rightarrow \Lambda\Lambda, \Lambda\Xi, \Lambda\bar{\Xi}, \Xi\Xi, \Sigma\Sigma, \Omega\Omega, \Lambda_c\Lambda_c, \Sigma_c\Sigma_c, \Omega_c\Omega_c$ can be produced allowing the study of the dependences on spin observables.



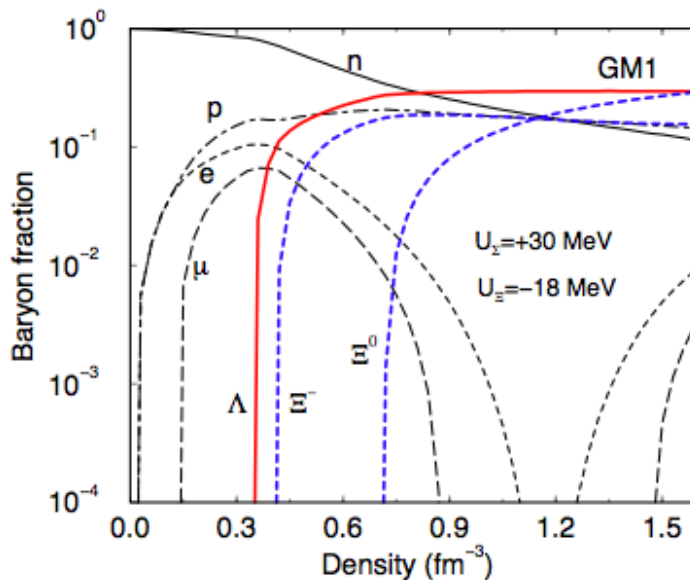
By comparing several reactions involving different quark flavours the OZI rule and its possible violation, can be tested

Channel 1.64 GeV/c	Rec. eff.	σ [μb]	Signal
$\bar{p}p \rightarrow \Lambda\bar{\Lambda}$	0.11	64	1
$\bar{p}p \rightarrow \bar{p}p\pi^+\pi^-$	$1.2 \cdot 10^{-5}$	~ 10	$4.2 \cdot 10^{-5}$
Channel 4 GeV/c			
$\bar{p}p \rightarrow \Lambda\bar{\Lambda}$	0.23	~ 50	1
$\bar{p}p \rightarrow \bar{p}p\pi^+\pi^-$	$< 3 \cdot 10^{-6}$	$3.5 \cdot 10^3$	$< 2.2 \cdot 10^{-3}$
$\bar{p}p \rightarrow \bar{\Lambda}\Sigma^0$	$5.1 \cdot 10^{-4}$	~ 50	$2.2 \cdot 10^{-3}$
$\bar{p}p \rightarrow \bar{\Lambda}\Sigma(1385)$	$< 3 \cdot 10^{-6}$	~ 50	$< 1.3 \cdot 10^{-5}$
$\bar{p}p \rightarrow \bar{\Sigma}^0\Sigma^0$	$< 3 \cdot 10^{-6}$	~ 50	$< 1.3 \cdot 10^{-5}$
Channel 15 GeV/c			
$\bar{p}p \rightarrow \Lambda\bar{\Lambda}$	0.14	~ 10	1
$\bar{p}p \rightarrow \bar{p}p\pi^+\pi^-$	$< 1 \cdot 10^{-6}$	$1 \cdot 10^3$	$< 2 \cdot 10^{-3}$
$\bar{p}p \rightarrow \bar{\Lambda}\Sigma^0$	$2.3 \cdot 10^{-3}$	~ 10	$1.6 \cdot 10^{-2}$
$\bar{p}p \rightarrow \bar{\Lambda}\Sigma(1385)$	$3.3 \cdot 10^{-5}$	60	$1.4 \cdot 10^{-3}$
$\bar{p}p \rightarrow \bar{\Sigma}^0\Sigma^0$	$3.0 \cdot 10^{-4}$	~ 10	$2.1 \cdot 10^{-3}$
DPM	$< 1 \cdot 10^{-6}$	$5 \cdot 10^4$	$< .09$
Channel 4 GeV/c			
Rec. eff.	σ (μb)	Signal	
$\bar{p}p \rightarrow \Xi^+\Xi^-$	0.19	~ 2	1
$\bar{p}p \rightarrow \bar{\Sigma}^+(1385)\Sigma^-(1385)$	$< 1 \cdot 10^{-6}$	~ 60	$< 2 \cdot 10^{-4}$



Baryon-baryon interaction

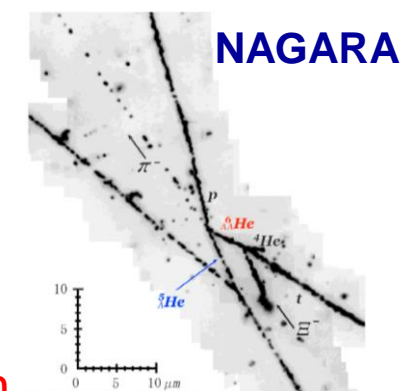
The knowledge of Baryon-Baryon potential is essential for the understanding of the composition of nuclear matter.



The fraction of baryons and leptons in neutron star matter [arXiv:0801.3791v1](https://arxiv.org/abs/0801.3791v1)

ΛΛ-hypernuclei, Ξ -atoms, Ω -atoms allow to have an insight to more complex nuclear systems containing strangeness (neutron stars, hyperon-stars, strange-quark stars, ...)

Nuclear NN forces are known, YN interaction, thanks to hypernuclear physics, is relatively known, but **YY interaction is completely unknown**, there are just a few double Λ hypernuclear events.



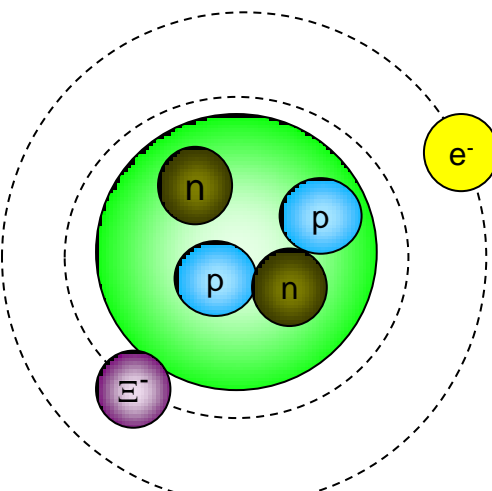


Double Strange Systems (DDS)

$(S=\pm 2)$ hyperon – antihyperon systems are fully accessible at PANDA

Exotic hyperatom:

Ξ^- occupies an atomic level

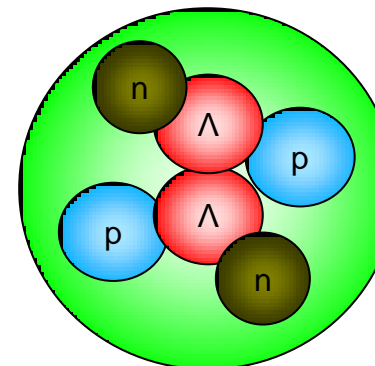


Ξ^- -nucleus interaction

- Atomic orbits overlap nucleus
- Strong interaction and Coulomb force interplay
- Lowest atomic levels are shifted and broadened
- Potential: Coulomb + optical

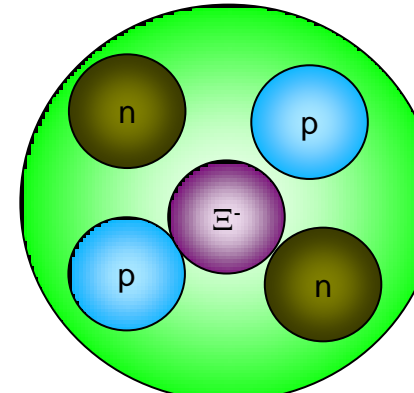
Double Λ Hypernucleus:

2 Λ 's replace 2 nucleons in a nucleus



Doubly Strange Hypernucleus:

Ξ^- occupies a nuclear level



$\Lambda\Lambda$ strong interaction

- only possible in double hypernuclei
- YY potential: attractive/repulsive?
- hyperfragments probability dependence on YY potential

One Boson Exchange features

$\Lambda\Lambda \rightarrow \Lambda\Lambda$: only non strange, $I=0$ meson exchange (ω, η, \dots)

$\Lambda\Lambda$ weak interaction: hyperon induced decay:

- $\Lambda\Lambda \rightarrow \Lambda n$: $\Gamma_{\Lambda n} \ll \Gamma_{\text{free}}$ (expected)
- $\Lambda\Lambda \rightarrow \Sigma^- p$: $\Gamma_{\Sigma p} \ll \Gamma_{\text{free}}$ (expected)

$\Xi^- N$ interaction:

- short range interaction
- long range interaction
-



A new way for double strange systems

- ✓ Up to now double strange systems have been produced by K^- beams in the reaction:

$K^- (N, \Xi^-) K^+$ (N- quasi free or bound in nucleus)

- S=-2 baryon can be produced via:



Goal:

maximize the “stopped Ξ^- ” with a suitable set-up

- ✓ Choice of the target:

free protons (hydrogen target) or protons and neutrons in a nucleus (quasi-free reactions)

- Advantages of nuclear target :

a) higher cross section (scaling as $\sim A^{2/3}$)

b) Ξ^- slowing down in dense (nuclear) matter

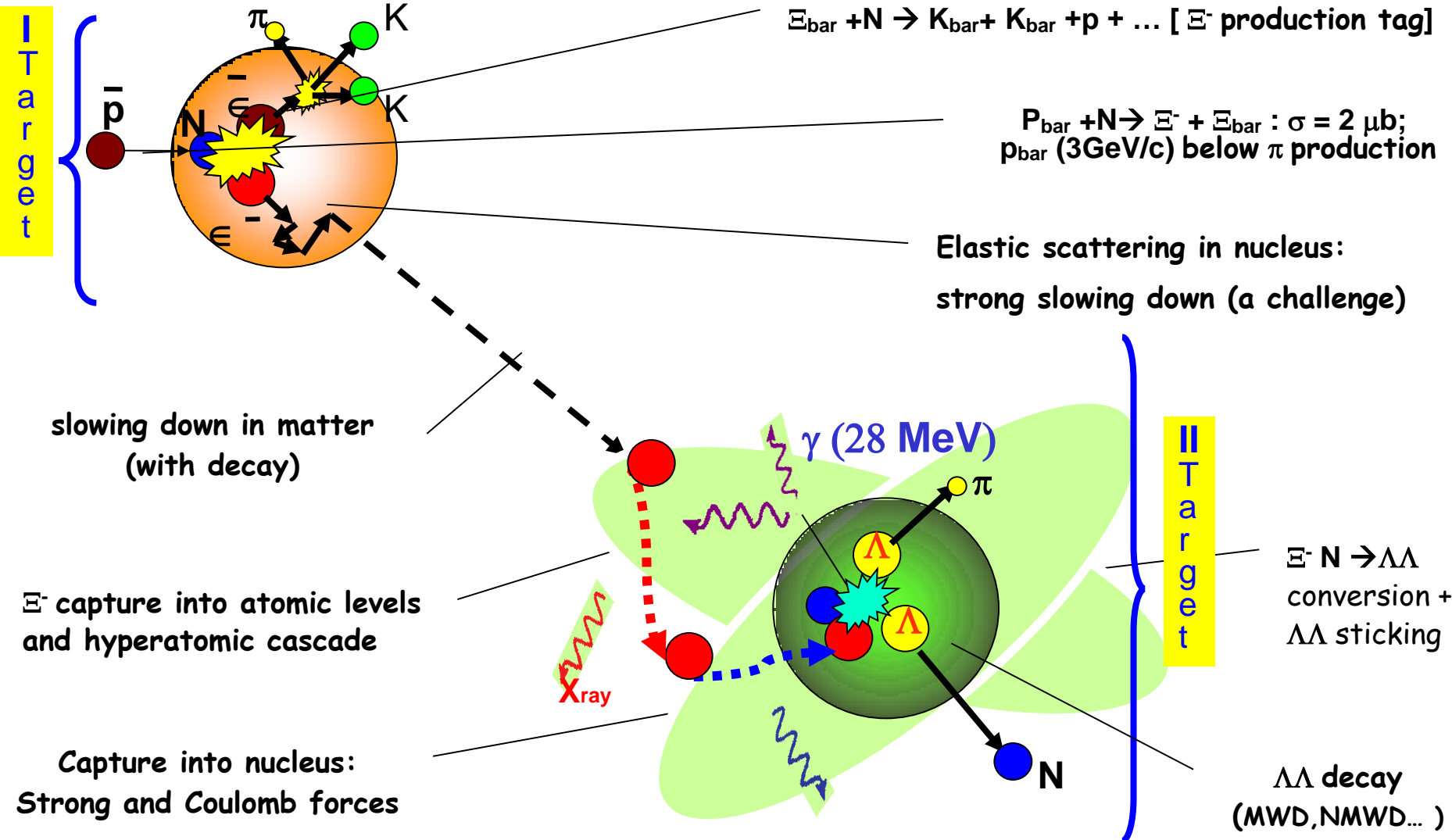
- Disadvantages of nuclear target :

c) high background (annihilation)

d) high beam consuming (beam losses)



A new way for double strange systems





$\Lambda\Lambda$ Hypernuclei

Status of the art:

Nucleus	$B_{\Lambda\Lambda}(\Lambda\Lambda^A Z)$ [MeV]	$\Delta B_{\Lambda\Lambda}(\Lambda\Lambda^A Z)$ [MeV]	Reference	Reaction
$\Lambda\Lambda^{10}\text{Be}$	17.7 ± 0.4	4.3 ± 0.4	M.Danysz et al., PRL.11(1963) 29	$K^- + A \rightarrow K^+ + \Xi^-$
$\Lambda\Lambda^6\text{He}$	10.9 ± 0.5	4.6 ± 0.5	D.J.Prowse, PRL.17(1966) 782	$K^- + A \rightarrow K^+ + \Xi^-$
$\Lambda\Lambda^{10}\text{Be}$	8.5 ± 0.7	-4.9 ± 0.7	KEK-E176	$K^- + p \rightarrow K^+ + \Xi^- (\text{q.f})$
$\Lambda\Lambda^{13}\text{B}$	27.6 ± 0.7	4.9 ± 0.7	S.Aoki et al., PTP.85(1991) 1287	$K^- + p \rightarrow K^+ + \Xi^- (\text{q.f})$
$\Lambda\Lambda^{12}\text{B}$		4.5 ± 0.5	P.Khaustov et al., PRC.61(2000)027601	$(^{12}\text{C})_{\text{atom}} \Xi^- \rightarrow ^{12}\text{B}_{\Lambda\Lambda} + n$
$\Lambda\Lambda^6\text{He}$	$7.25 \pm 0.19^{+0.18}_{-0.11}$	$1.01 \pm 0.2^{+0.18}_{-0.11}$	KEK-E373,NAGARA H.Takahashi et al., PRL.87(2001)212502-1	$K^- + p \rightarrow K^+ + \Xi^- (\text{q.f})$
$\Lambda\Lambda^{12}\text{B}$		$\sigma(\theta < 8^\circ) \approx 6-10\text{nb}$	K.Yamamoto et al., PLB.478(2000) 401	$K^- + ^{12}\text{C} \rightarrow K^+ + ^{12}\text{B}_{\Lambda\Lambda}$

Up to know these systems have been studied in cosmic rays or using kaon-beams:



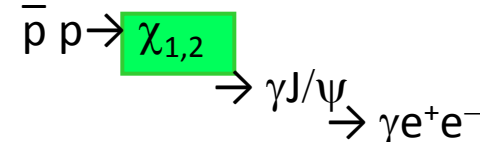
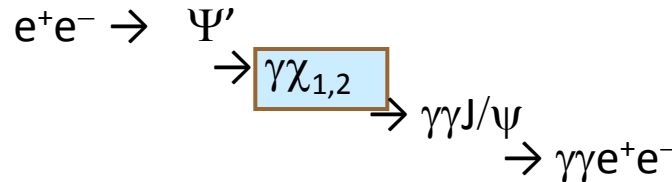
KEK, BNL-AGS, have demonstrated that the systems are produced.

At JPARC with high intensity kaon-beams the goal is to stop $10^4 \Xi^-$ in a nuclear target.

At PANDA the same amount of data will be collected, with the possibility to run with different nuclear targets at the same time.



Antiproton power



- e^+e^- interactions:

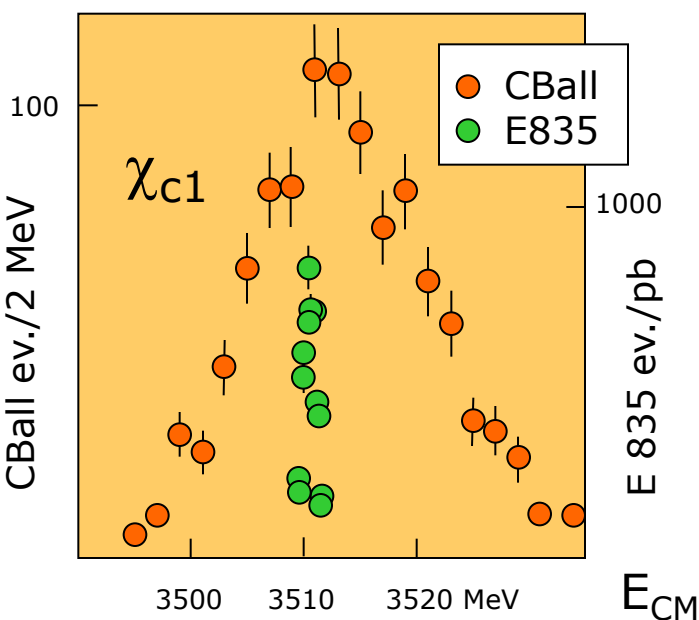
- Only 1^{--} states are formed
- Other states only by secondary decays (moderate mass resolution related to the detector)

- $\bar{p}p$ reactions:

- Most states directly formed (very good mass resolution; \bar{p} -beam can be efficiently cooled)

$$\text{Br}(p\bar{p} \rightarrow \eta_c) = 1.2 \cdot 10^{-3}$$

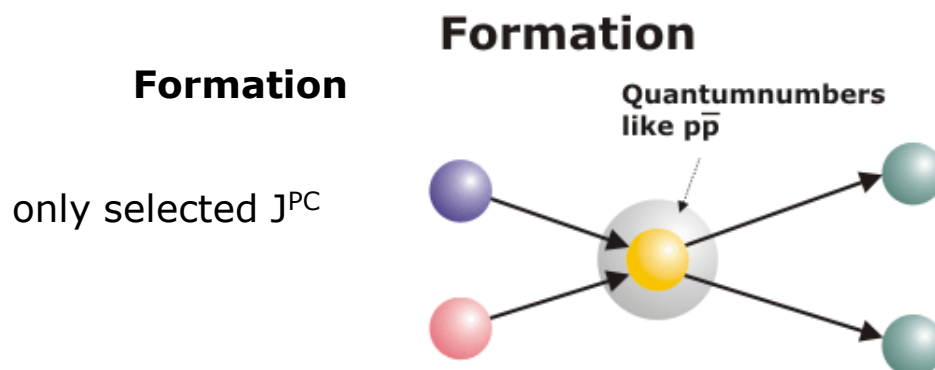
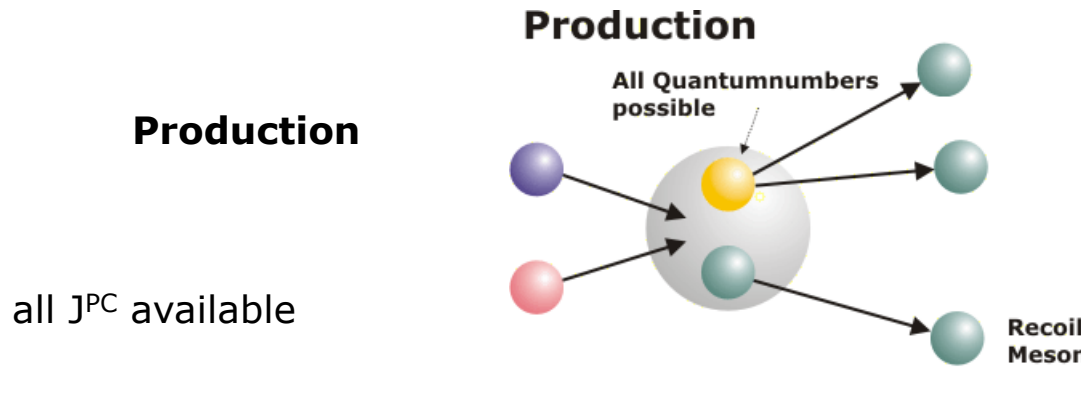
$$\text{Br}(e^+e^- \rightarrow \psi) \cdot \text{Br}(\psi \rightarrow \gamma\eta_c) = 2.5 \cdot 10^{-5}$$





Spectroscopy with antiprotons

There are two mechanisms to access particular final states:

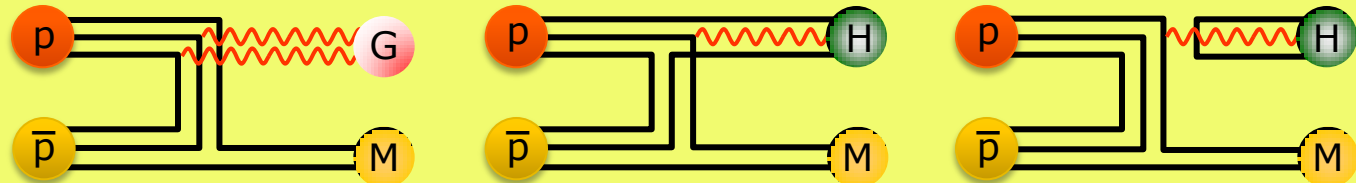




Spectroscopy with antiprotons

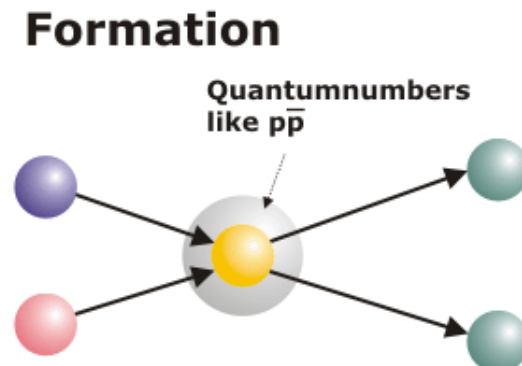
There are two mechanisms to access particular final states:

Production



Even exotic quantum numbers
can be reached $\sigma \sim 100 \text{ pb}$

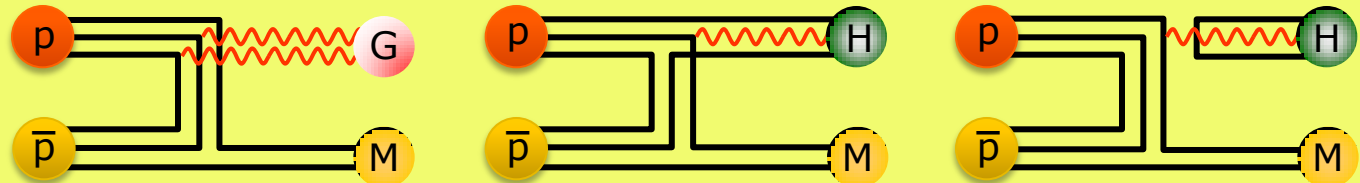
Formation
only selected J^{PC}





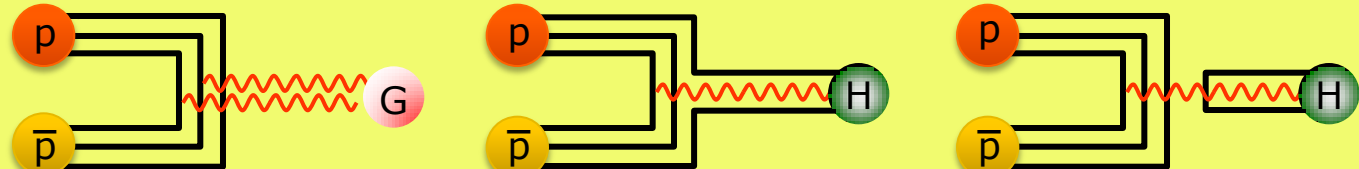
Spectroscopy with antiprotons

Production



Even exotic quantum numbers
can be reached $\sigma \sim 100 \text{ pb}$

Formation



All ordinary quantum numbers
can be reached $\sigma \sim 1 \mu\text{b}$



Exotic hadrons

The QCD spectrum is much rich than that of the naive quark model also the gluons can act as hadron components

The “exotic hadrons” fall in 3 general categories:

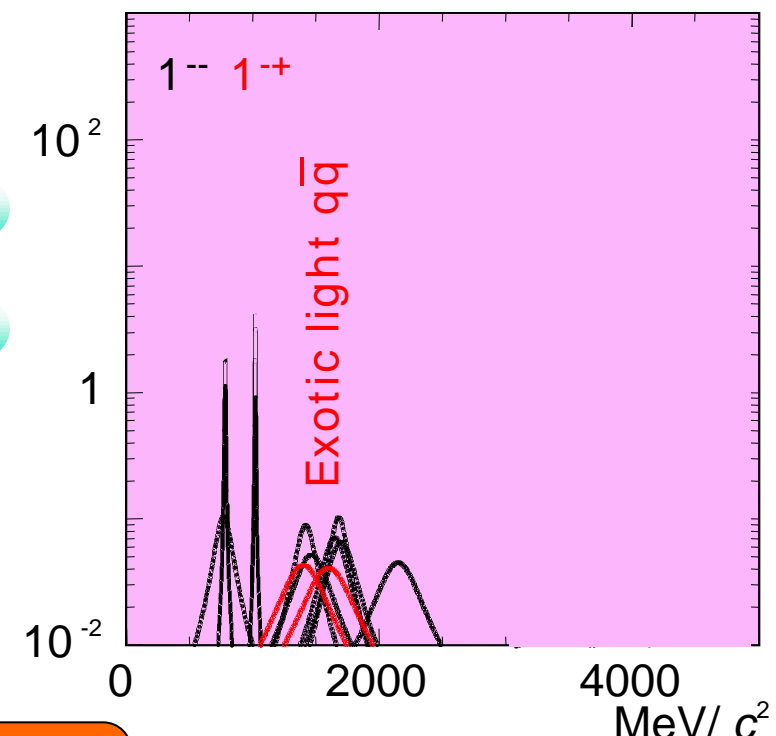
Multiquarks $(qq)(qq)$



Hybrids $(qq) g$



Glueballs gg



In the light meson spectrum exotic states overlap with conventional states



Exotic hadrons

The QCD spectrum is much rich than that of the naive quark model also the gluons can act as hadron components

The “exotic hadrons” fall in 3 general categories:

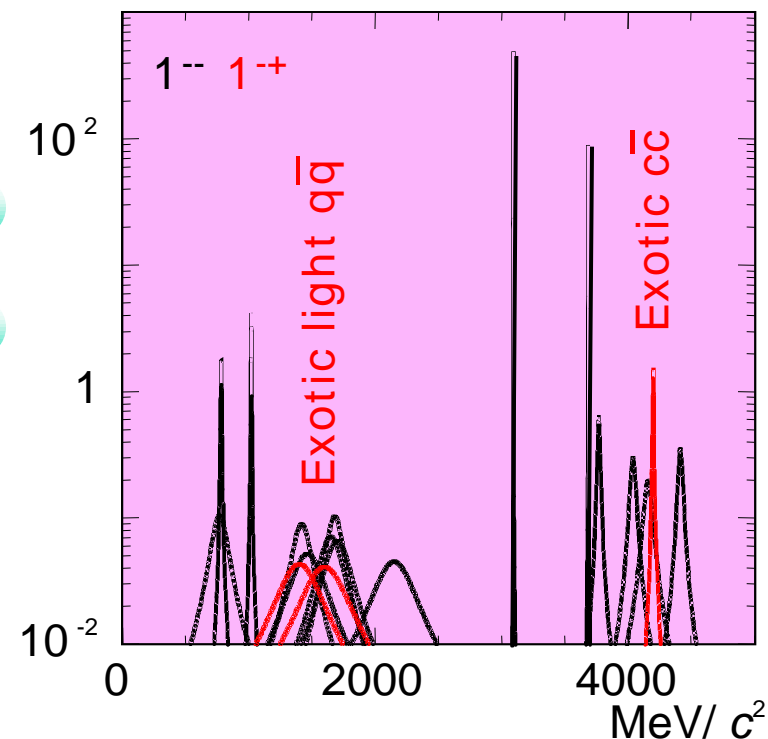
Multiquarks $(qq)(qq)$



Hybrids $(qq) g$



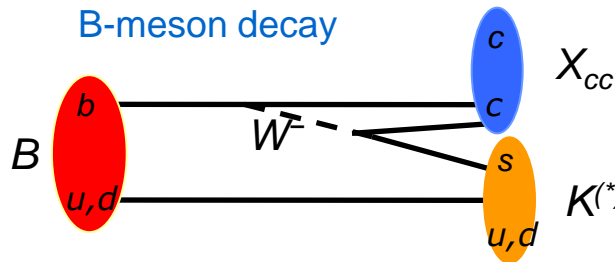
Glueballs gg



In the $\bar{c}c$ meson spectrum the density of states is lower and therefore so the overlap



XYZ Mesons



X(3872) Belle, Babar, Cleo, CDF, D0

Y(3940) Belle, Babar

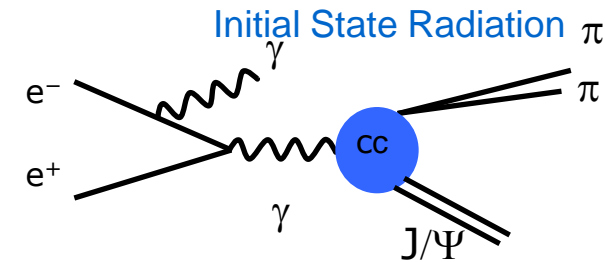
Y(4140)? CDF

Z(4430)

Z₁(4050)

Z₂(4250)

Belle



1-- states

X(4008)? Belle

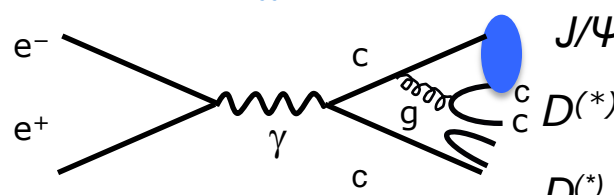
Y(4260) BaBar, Belle, CLEO

Y(4350) BaBar, Belle

Y(4660) Belle

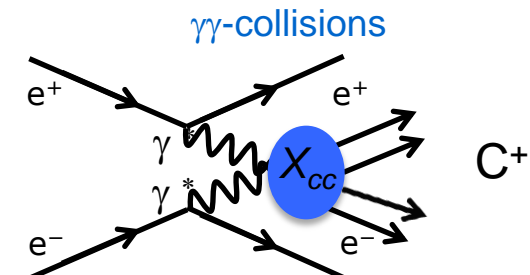
Associate production

$e^+ e^- \rightarrow J/\Psi X_{cc}$



X(3940) Belle
X(4160) Belle

X(3915) Belle
Z(3930) Belle
Y(4350) Belle

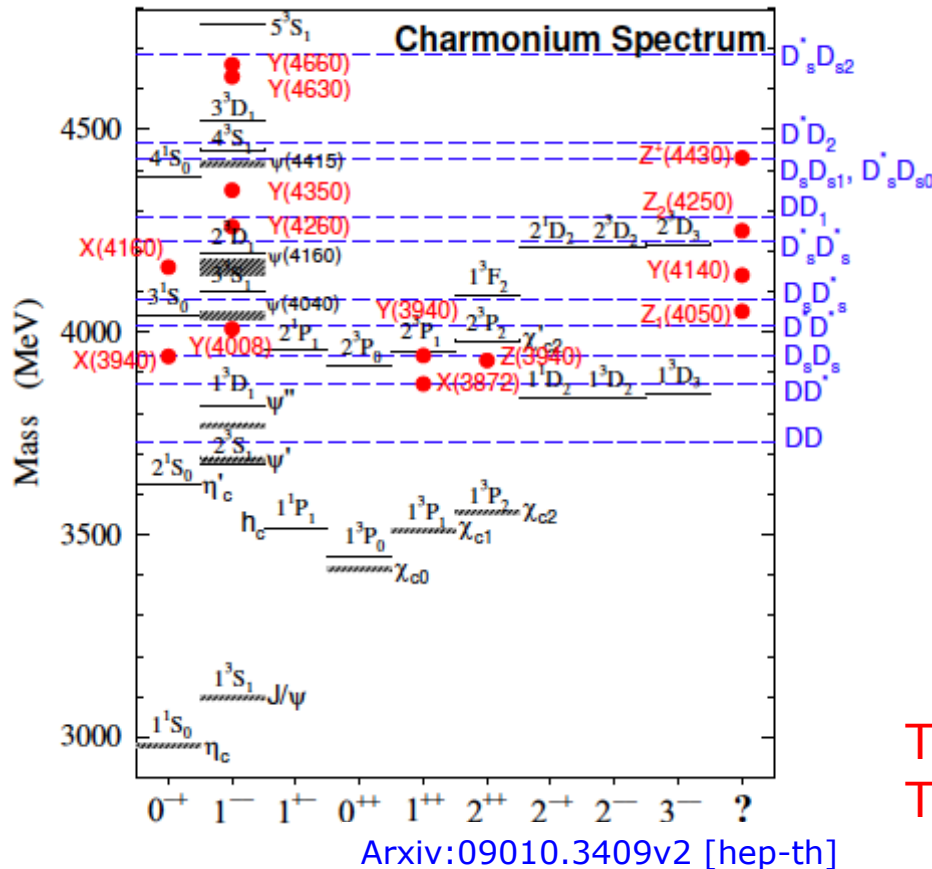


The B-factory experiments have discovered a large number of candidates for charmonium and charmonium-like meson states, many of which can not be easily accommodated by theory. State parameters are still largely unknown. Few events collected in 10 years of running
PANDA will detect 100 events per day



XYZ Mesons

Without entering into the details of each state some general consideration can be drawn.



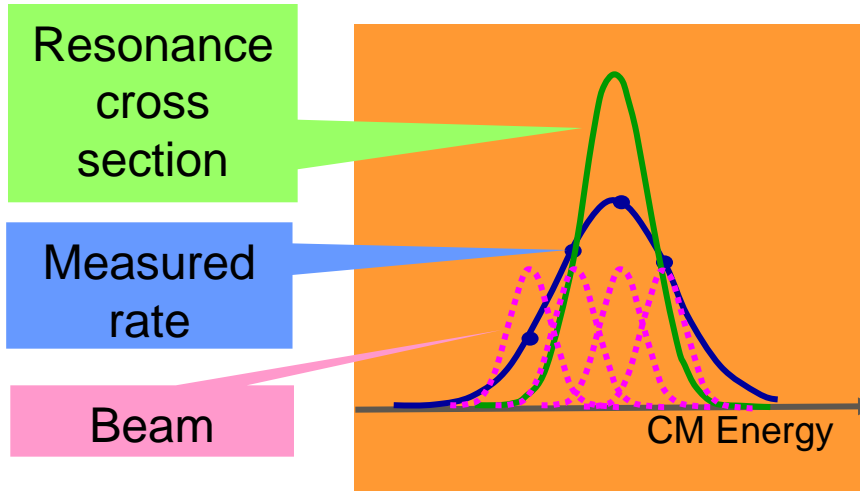
- masses are barely known;
- often widths are just upper limits;
- few final states have been studied;
- statistics are poor;
- quantum number assignment is possible for few states;
- some resonances need confirmation...

There are problems of compatibility Theory - Experiment

Quantum numbers assignment and structure become clear only with high statistics, different final states and very precise energy measurements.,



Antiproton power



- e^+e^- : typical mass res. ~ 10 MeV
- Fermilab: 240 keV
- HESR: ~ 30 keV

The production rate of a certain final state v is a convolution of the BW cross section and the beam energy distribution function $f(E, \Delta E)$:

$$v = L_0 \left\{ \mathcal{E} \int dE f(E, \Delta E) \sigma_{BW}(E) + \sigma_b \right\}$$

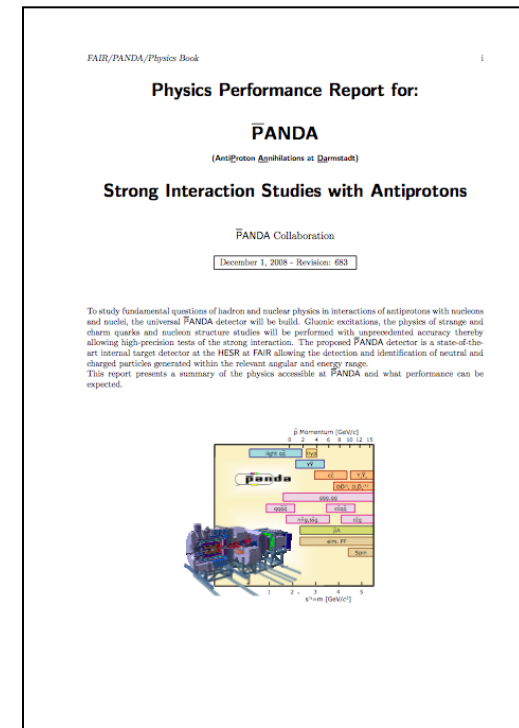
The resonance mass M_R , total width Γ_R and product of branching ratios into the initial and final state $B_{in}B_{out}$ can be extracted by measuring the formation rate for that resonance as a function of the cm energy E .



PANDA Physics Performance Report

All the details of the PANDA experimental program are reported in the "Physics Performance Report".

Within this document, we present the results of detailed simulations performed to evaluate detector performance on many benchmark channels.



arXiv:0903.3905v1



on behalf of the PANDA Collaboration
THANK YOU!



Drell-Yan Asymmetries — $\bar{p}p \rightarrow \mu^+ \mu^- X$

Di-Lepton Rest Frame

$$\frac{1}{\sigma} \frac{d\sigma}{d\Omega} = \frac{3}{4\pi} \frac{1}{\lambda + 3} \left(1 + \lambda \cos^2 \theta + \mu \sin^2 \theta \cos \varphi + \frac{\nu}{2} \sin^2 \theta \cos 2\varphi \right)$$

NLO pQCD: $\lambda \sim 1$, $\mu \sim 0$, $\nu \sim 0$

Lam-Tung sum rule: $1 - \lambda = 2\nu$

- reflects the spin- $1/2$ nature of the quarks
- insensitive top QCD-corrections

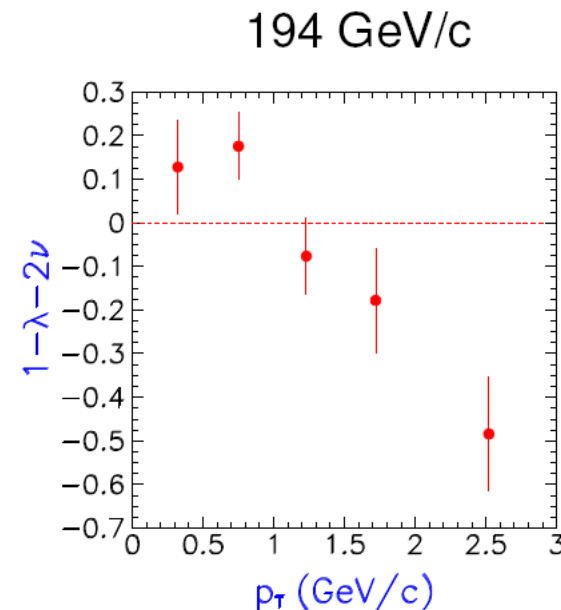
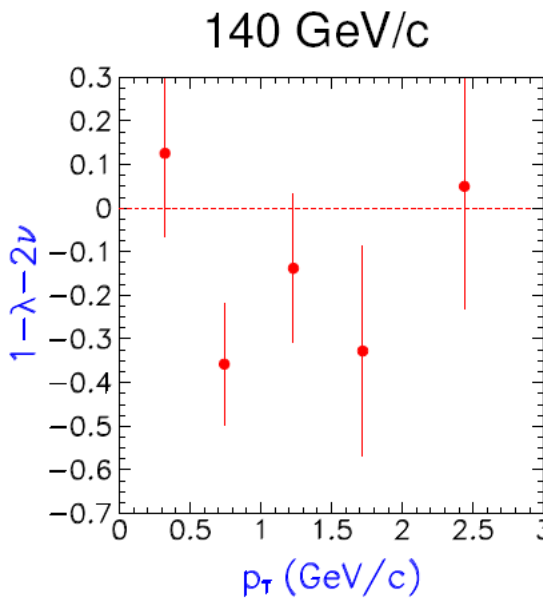
Experimental data ^[1]: $\nu \sim 30\%$

^[1] J.S.Conway et al., Phys. Rev. D39 (1989) 92.

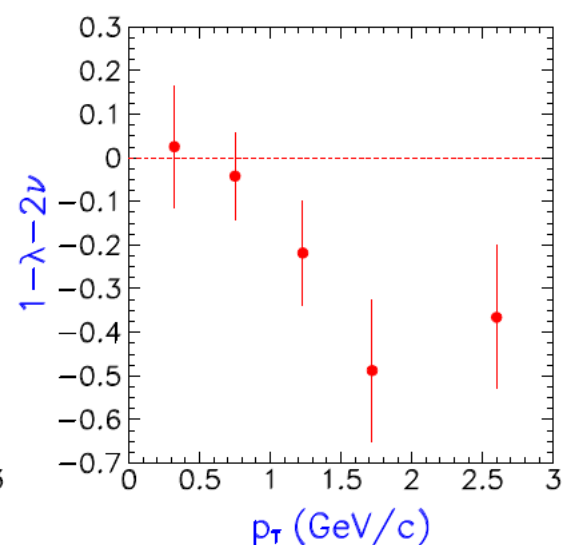


Remarkable and unexpected violation of Lam-Tung rule

λ, μ, ν measured in $\pi N \rightarrow \mu^+ \mu^- X$



NA10 @ CERN



ν involves transverse spin effects at leading twist [2]

If unpolarised DY σ is kept differential on k_T ,
cos2 φ contribution to angular distribution provide:

$$h_1^\perp(x_2, \kappa_\perp^2) \times \bar{h}_1^\perp(x_1, \kappa_\perp'^2)$$

[2] D. Boer et al., Phys. Rev. D60 (1999) 014012.

[1] NA10 coll., Z. Phys. C37 (1988) 545

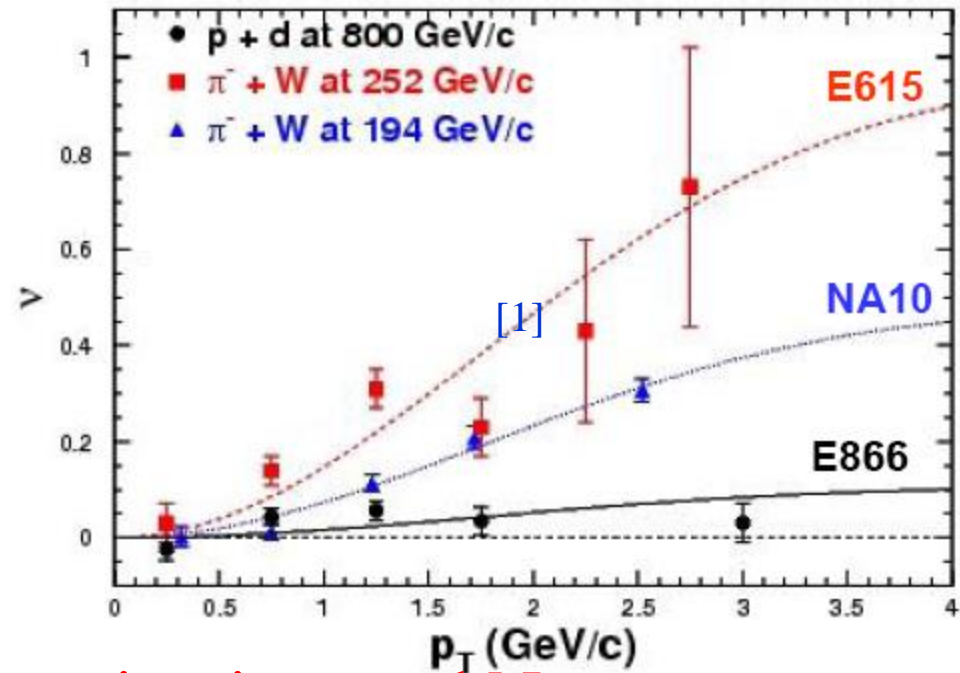


Drell-Yan Asymmetries — $\bar{p}p \rightarrow \mu^+ \mu^- X$

Boer-Mulders

$$h_1^\perp = \text{circle with arrow down} - \text{circle with arrow up}$$

T-odd Chiral-odd TMD



- $v > 0 \rightarrow$ valence h_1^\perp has same sign in π and N
- $v(\pi^- W \rightarrow \mu^+ \mu^- X) \sim h_1^\perp(\pi)_{\text{valence}} \times h_1^\perp(p)_{\text{valence}}$
- $v(p d \rightarrow \mu^+ \mu^- X) \sim h_1^\perp(p)_{\text{valence}} \times h_1^\perp(p)_{\text{sea}}$
- $v > 0 \rightarrow$ valence and sea h_1^\perp has same sign, but sea h_1^\perp should be significantly smaller

[1] L. Zhu et al, PRL 99 (2007) 082301;

[12] D. Boer, Phys. Rev. D60 (1999) 014012.



Transverse Single Spin Asymmetries: correlation functions

All these effects may lead to
Single Spin Asymmetries (SSA):

$$A_N = \frac{d\sigma^{\uparrow} - d\sigma^{\downarrow}}{d\sigma^{\uparrow} + d\sigma^{\downarrow}}$$

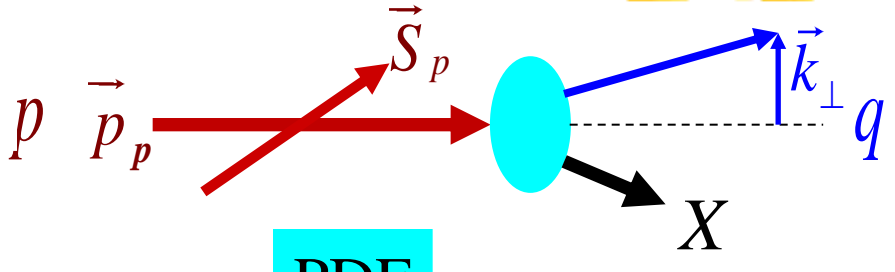


Transverse Single Spin Asymmetries: correlation functions

Sivers effect

of partons in polarized proton depends on

$$\vec{S}_p \cdot (\vec{p}_p \times \vec{k}_\perp)$$



part $f_{q/p,S}(x, \mathbf{k}_\perp) = f_{q/p}(x, \mathbf{k}_\perp) - \frac{k_\perp}{M} f_{1T}^{\perp q}(x, \mathbf{k}_\perp) \mathbf{S} \cdot (\hat{\mathbf{p}} \times \hat{\mathbf{k}}_\perp)$

$\hookrightarrow q - (P_q \wedge n^\perp)$

Collins effect

fr $f_{q,s_q/p}(x, \mathbf{k}_\perp) = \frac{1}{2} f_{q/p}(x, \mathbf{k}_\perp) - \frac{1}{2} \frac{k_\perp}{M} h_1^{\perp q}(x, \mathbf{k}_\perp) \mathbf{s}_q \cdot (\hat{\mathbf{p}} \times \hat{\mathbf{k}}_\perp)$

FF

Polarising Fragmentation Function

$D_{h/q,s_q}(z, \mathbf{p}_\perp) = D_{h/q}(z, \mathbf{p}_\perp) + \frac{p_\perp}{z M_h} H_1^{\perp q}(z, \mathbf{p}_\perp) \mathbf{s}_q \cdot (\hat{\mathbf{p}}_q \times \hat{\mathbf{p}}_\perp)$

$\hookrightarrow \Lambda$

$\vec{S}_\Lambda \cdot (\vec{p}_q \times \vec{p}_\perp)$

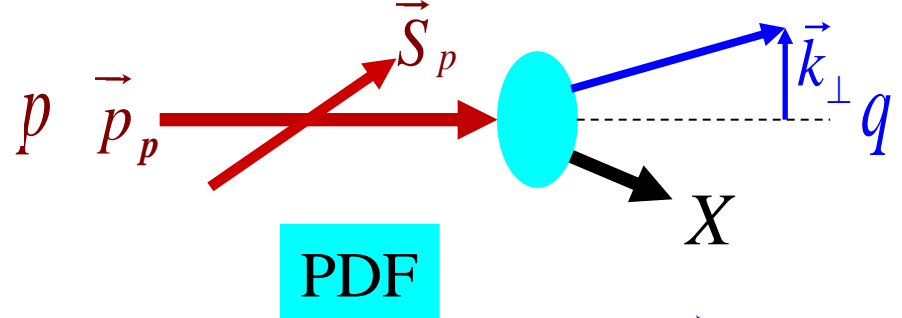


Transverse Single Spin Asymmetries: correlation functions

Sivers effect

of partons in polarized proton depends on

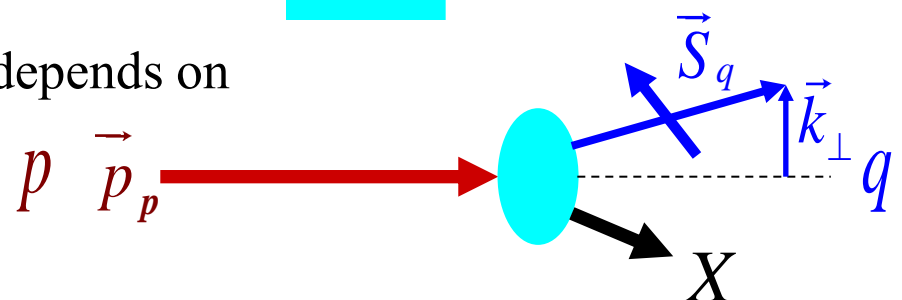
$$\vec{S}_p \cdot (\vec{p}_p \times \vec{k}_\perp)$$



Boer – Mulders effect

partons' polarisation in unpolarized proton depends on

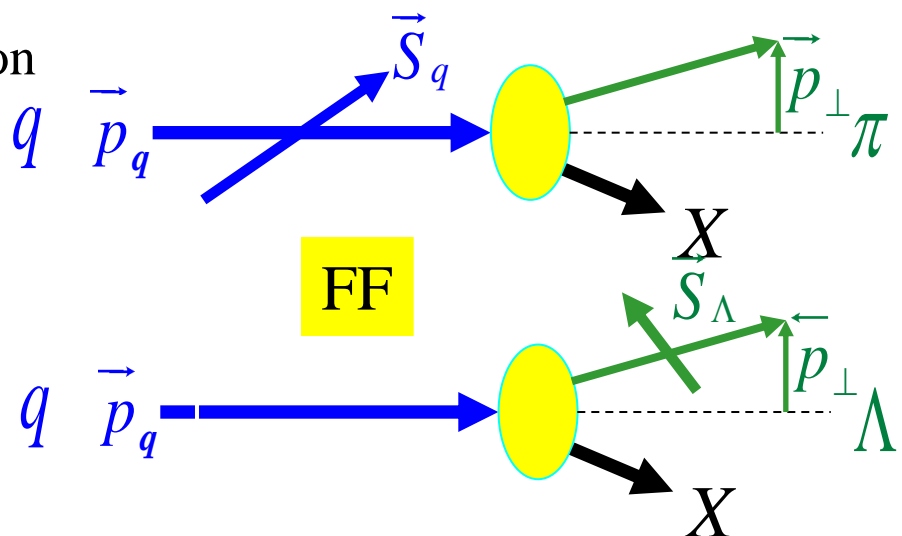
$$\vec{S}_q \cdot (\vec{p}_q \times \vec{k}_\perp)$$



Collins effect

fragmentation of polarised quark depends on

$$\vec{S}_q \cdot (\vec{p}_q \times \vec{p}_\perp)$$



Polarising Fragmentation Function

Hadrons' polarisation coming from

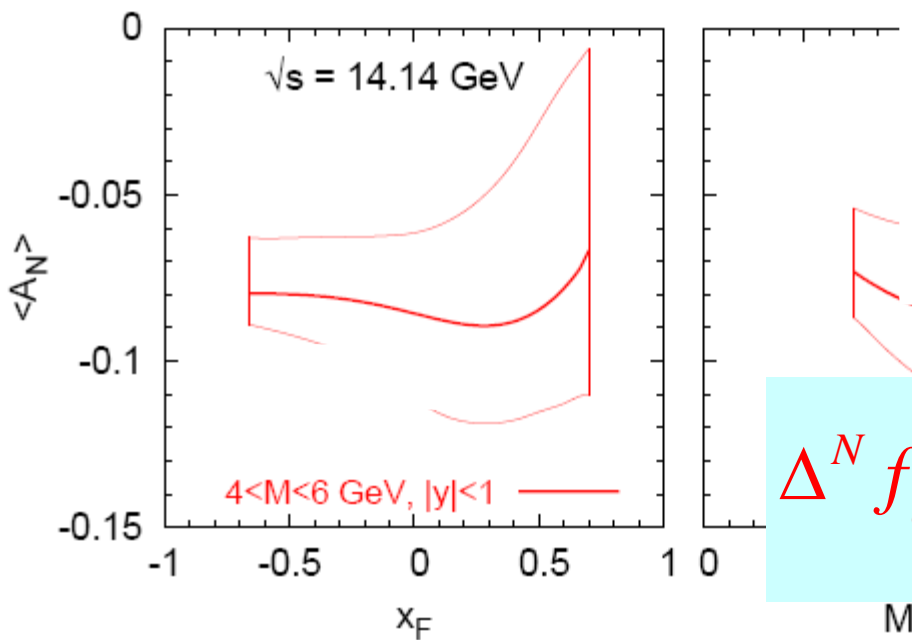
Unpolarised quarks depends on

$$\vec{S}_\Lambda \cdot (\vec{p}_q \times \vec{p}_\perp)$$



Transverse Single Spin Asymmetries in Drell-Yan

$$A_N = \frac{d\sigma^{\uparrow} - d\sigma^{\downarrow}}{d\sigma^{\uparrow} + d\sigma^{\downarrow}}$$



expected^[1] to be small but not negligible
for HESR layout on fixed target

Test of Universality

$$f_{1T}^{\perp q}(x, k_{\perp})_{SIDIS} = -f_{1T}^{\perp q}(x, k_{\perp})_{DY} \quad [2]$$

$\Delta^N f_{q/p\uparrow}(x_q, k_{\perp q}) = -\frac{2k_{\perp}}{m_p} f_{1T}^{\perp q}(x, k_{\perp})$

$\sqrt{s} = 14.14 \text{ GeV}$

$M (\text{GeV})$

Originates from the Sivers function^[1]:

$$A_N = \frac{\sum_q e_q^2 \int d^2 \mathbf{k}_{\perp q} d^2 \mathbf{k}_{\perp \bar{q}} \delta^2(\mathbf{k}_{\perp q} + \mathbf{k}_{\perp \bar{q}} - \mathbf{q}_T) \Delta^N f_{q/p\uparrow}(x_q, \mathbf{k}_{\perp q}) f_{\bar{q}/p}(x_{\bar{q}}, \mathbf{k}_{\perp \bar{q}})}{2 \sum_q e_q^2 \int d^2 \mathbf{k}_{\perp q} d^2 \mathbf{k}_{\perp \bar{q}} \delta^2(\mathbf{k}_{\perp q} + \mathbf{k}_{\perp \bar{q}} - \mathbf{q}_T) f_{q/p}(x_q, \mathbf{k}_{\perp q}) f_{\bar{q}/p}(x_{\bar{q}}, \mathbf{k}_{\perp \bar{q}})}$$

^[1] Anselmino et al., Phys. Rev. D72, 094007 (2005).

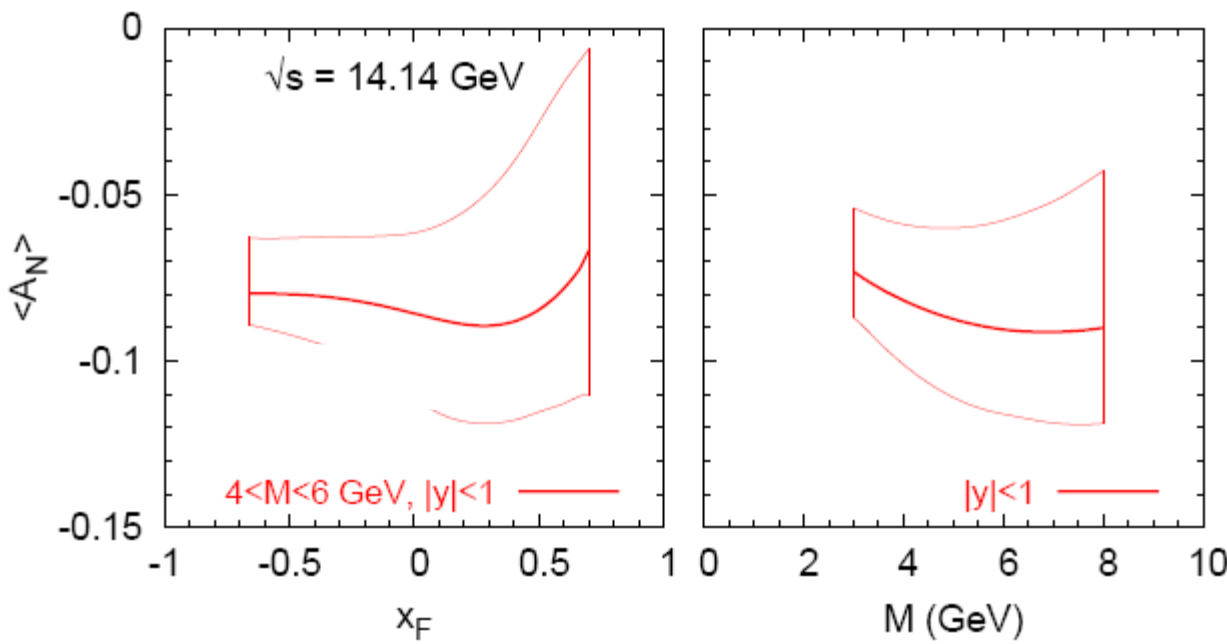
^[2] J.C. Collins, Phys. Lett. B536 (2002) 43



Transverse Single Spin Asymmetries in Drell-Yan

$$A_N = \frac{d\sigma^{\uparrow} - d\sigma^{\downarrow}}{d\sigma^{\uparrow} + d\sigma^{\downarrow}}$$

expected^[1] to be small but not negligible
for HESR layout on fixed target



$$0 \leq q_T \leq 1 \text{ GeV}/c$$

$$\sqrt{s} = 14.14 \text{ GeV}$$

Originates from the Sivers function^[1]:

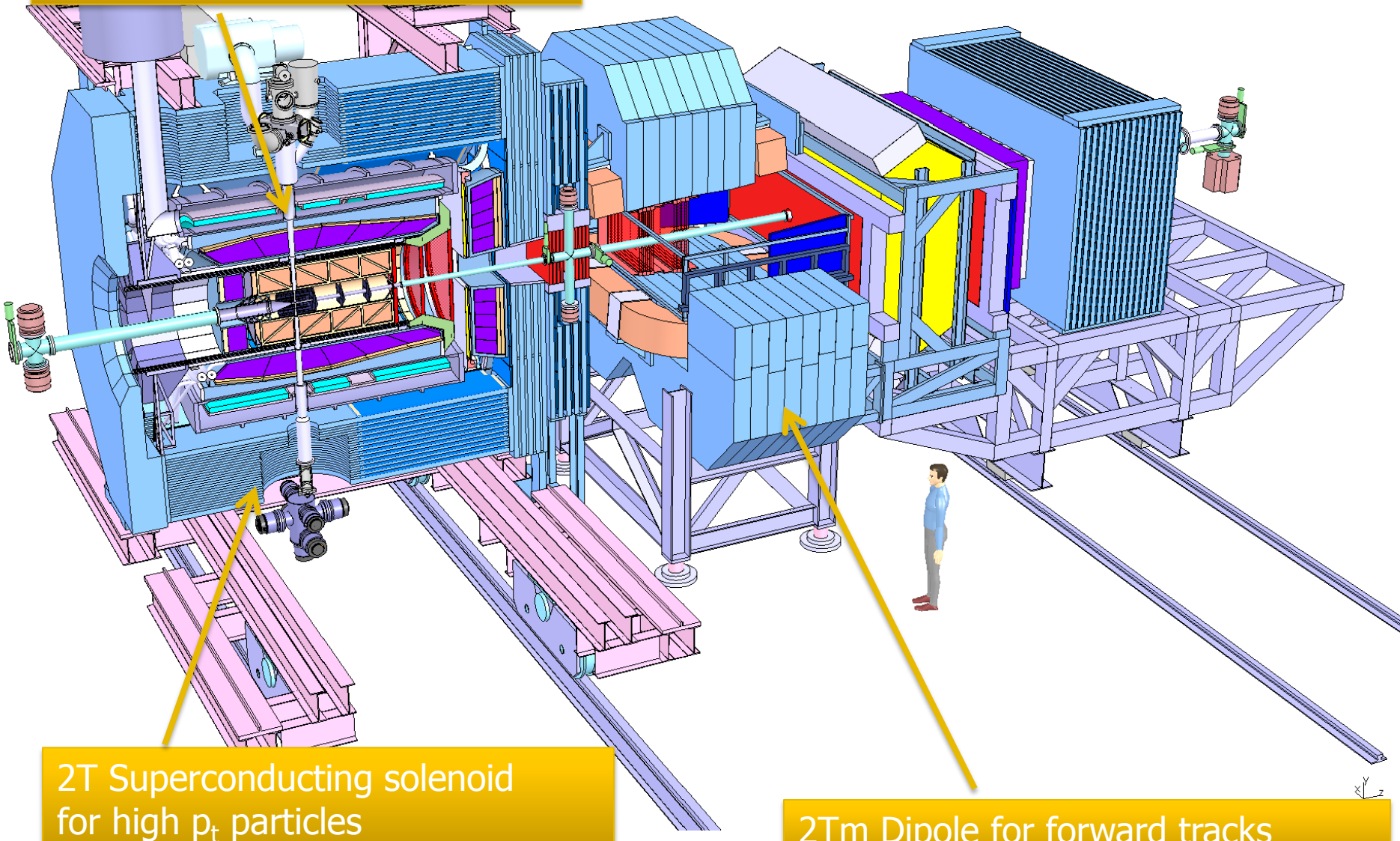
$$A_N = \frac{\sum_q e_q^2 \int d^2 \mathbf{k}_{\perp q} d^2 \mathbf{k}_{\perp \bar{q}} \delta^2(\mathbf{k}_{\perp q} + \mathbf{k}_{\perp \bar{q}} - \mathbf{q}_T) \Delta^N f_{q/p\uparrow}(x_q, \mathbf{k}_{\perp q}) f_{\bar{q}/p}(x_{\bar{q}}, \mathbf{k}_{\perp \bar{q}})}{2 \sum_q e_q^2 \int d^2 \mathbf{k}_{\perp q} d^2 \mathbf{k}_{\perp \bar{q}} \delta^2(\mathbf{k}_{\perp q} + \mathbf{k}_{\perp \bar{q}} - \mathbf{q}_T) f_{q/p}(x_q, \mathbf{k}_{\perp q}) f_{\bar{q}/p}(x_{\bar{q}}, \mathbf{k}_{\perp \bar{q}})}$$

^[1] Anselmino et al., Phys. Rev. D72, 094007 (2005).

^[2] J.C. Collins, Phys. Lett. B536 (2002) 43

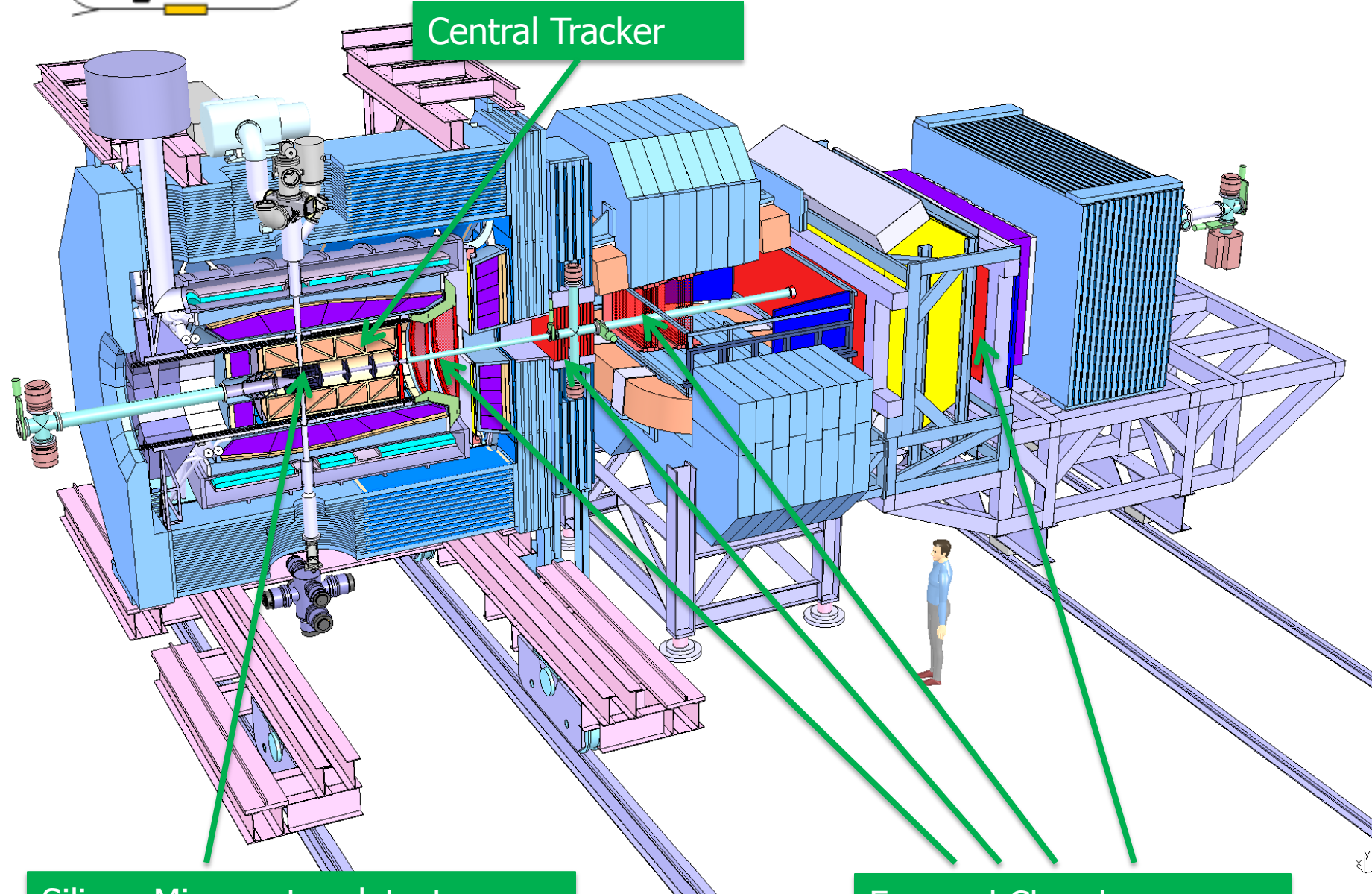


Pellet or cluster-jet target





panda

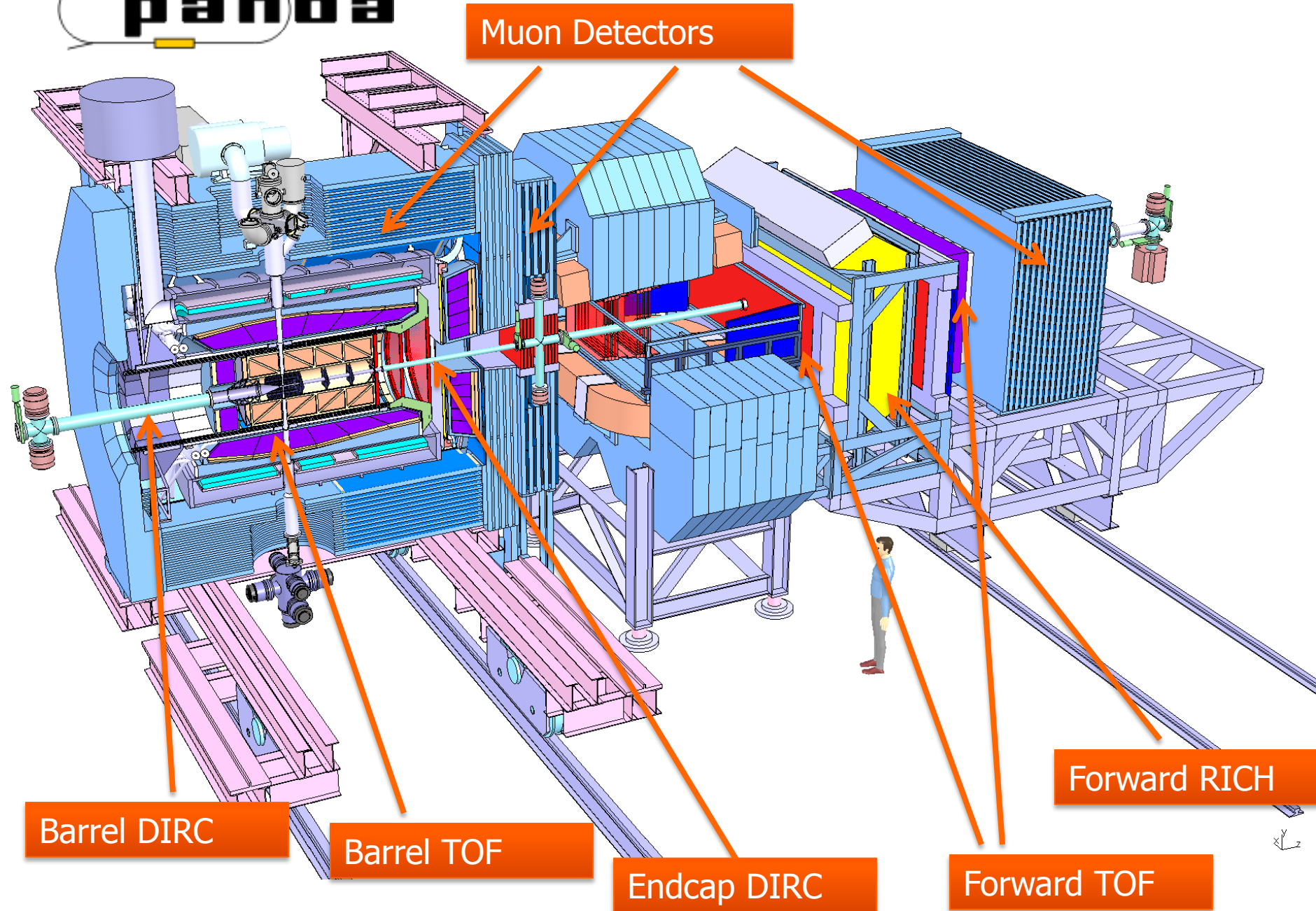


Silicon Microvertex detector

Forward Chambers

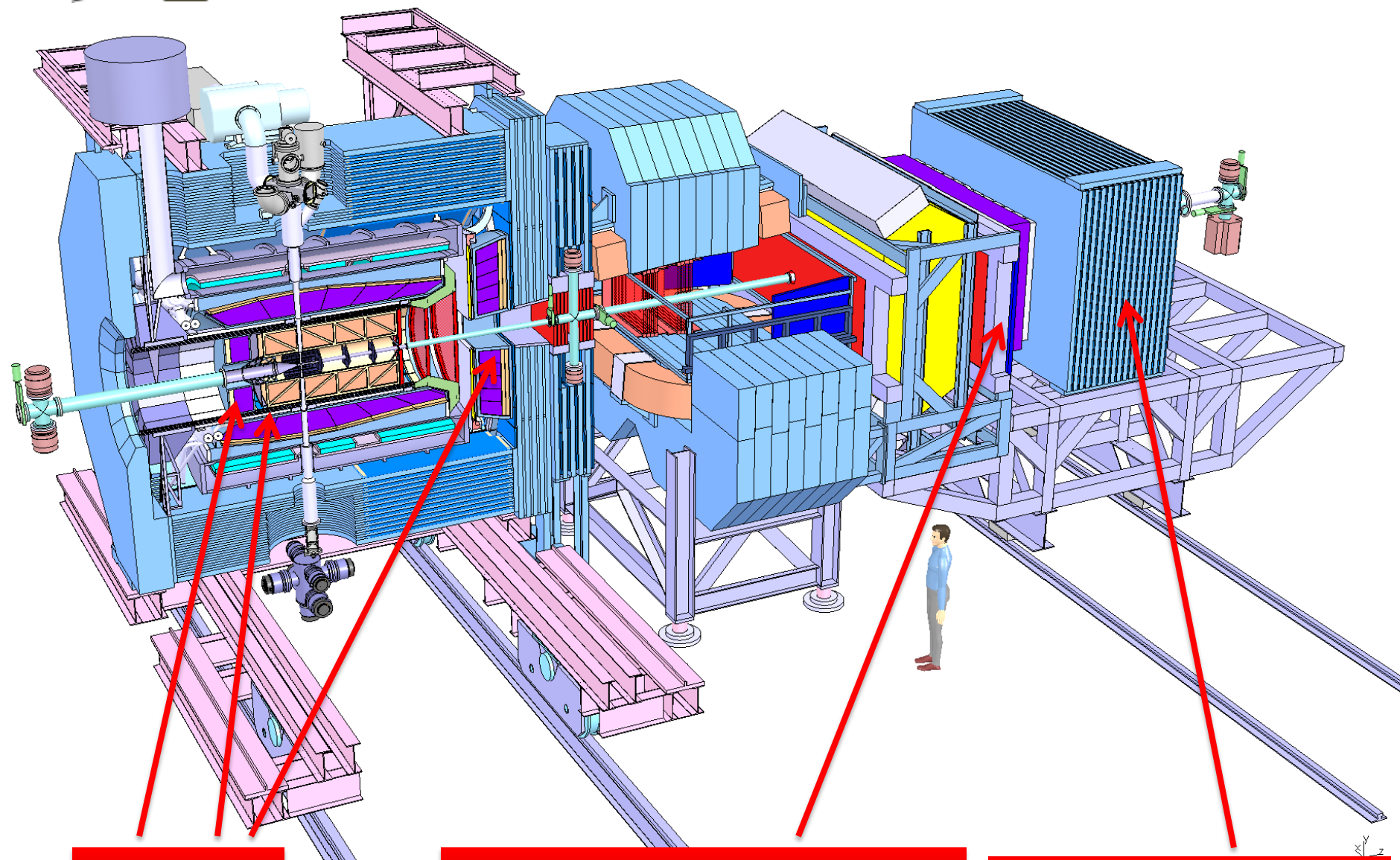


panda





panda



PWO EMC

Forward Shashlyk EMC

Hadron Calorimeter